

# Bio-Electrochemical Cell Assisted Production of Biogenic Palladium Nanoparticles with *Shewanella oneidensis* MR-1 Bacteria for the Catalytic Removal of Ofloxacin (OFX) and Doxycycline (DOX) Micropollutants in Pharmaceutical Industry Wastewaters

Rukiye Oztekin, Delia Teresa Sponza \*

Dokuz Eylül University, Engineering Faculty, Department of Environmental Engineering, Tınaztepe Campus, 35160 Buca/Izmir, Turkey.

\*Corresponding Author: Delia Teresa Sponza, Dokuz Eylül University, Engineering Faculty, Department of Environmental Engineering, Tınaztepe Campus, 35160 Buca/Izmir, Turkey.

Received Date: March 01, 2023 | Accepted Date: March 22, 2023 | Published Date: April 04, 2023

**Citation:** Oztekin R., Delia T. Sponza, (2023), Bio-Electrochemical Cell Assisted Production of Biogenic Palladium Nanoparticles with *Shewanella oneidensis* MR-1 Bacteria for the Catalytic Removal of Ofloxacin (OFX) and Doxycycline (DOX) Micropollutants in Pharmaceutical Industry Wastewaters, *International Journal of Clinical Case Reports and Reviews*, 13(4); DOI: 10.31579/2690-4861/300

**Copyright:** © 2023, Delia Teresa Sponza. This is an open-access article distributed under the terms of the Creative Commons Attribution License, which permits unrestricted use, distribution, and reproduction in any medium, provided the original author and source are credited.

## Abstract:

In this study, biogenic-palladium nanoparticles (bio-Pd NPs) with *Shewanella oneidensis* MR-1 bacteria as a heterostructure bio-electrochemical cell catalysts was examined during catalytic degradation process in the efficient removal of Ofloxacin (OFX) and Doxycycline (DOX) micropollutants from pharmaceutical industry wastewater plant, İzmir, Turkey. Different pH values (3.0, 4.0, 6.0, 7.0, 9.0 and 11.0), increasing micropollutants (OFX and DOX) concentrations (5 mg/l, 15 mg/l, 30 mg/l and 45 mg/l), increasing Bio-Pd NPs concentrations (5 mg/l, 10 mg/l, 20 mg/l, 30 mg/l, 40 mg/l and 60 mg/l), different Bio-Pd NPs/cell dry weight (CDW) mass ratios (5/5, 6/4, 7/3, 8/2, 9/1, 1/9, 2/8, 3/7 and 4/6), increasing recycle times (1., 2., 3., 4., 5., 6. and 7.) was operated during catalytic degradation process in the efficient removals of OFX and DOX micropollutants in pharmaceutical industry wastewater. The characteristics of the synthesized NPs were assessed using Diffuse reflectance UV-Vis spectra (DRS), Energy-dispersive X-ray (EDX), Field emission scanning electron microscopy (FESEM), Fourier transform infrared spectroscopy (FTIR), Inductively coupled plasma mass spectrometry (ICP-MS), Transmission Electron Microscopy (TEM), X-Ray Diffraction (XRD) and X-Ray Photoelectron Spectroscopy (XPS) analyses, respectively. The catalytic activity was first assessed by the degradation of methyl orange. The Bio-NPs showing the highest catalytic activity were selected for the removal of micropollutants (OFX and DOX) from secondary treated municipal wastewater. The catalytic degradation mechanisms of bio-Pd NPs with *Shewanella oneidensis* MR-1 bacteria as a heterostructure bio-electrochemical cell catalysts and the reaction kinetics of OFX and DOX micropollutants were evaluated in pharmaceutical industry wastewater during catalytic degradation process. ANOVA statistical analysis was used for all experimental samples. The maximum 99% OFX removal efficiency was obtained catalytic removals with bio-electrochemical cell assisted production of bio-Pd NPs with *Shewanella oneidensis* MR-1 bacteria bio-electrochemical cell catalysts in pharmaceutical industry wastewater, at 30 mg/l OFX concentration, 40 mg/l Bio-Pd NPs concentration, Bio-Pd NPs/CDW mass ratio=6/4, after 24 h catalytic degradation time, at pH=6.0, at 25°C, respectively. The maximum 99% DOX removal efficiency was observed catalytic removals with bio-electrochemical cell assisted production of bio-Pd NPs with *Shewanella oneidensis* MR-1 bacteria bio-electrochemical cell catalysts in pharmaceutical industry wastewater, at 30 mg/l DOX concentration, 40 mg/l Bio-Pd NPs concentration, Bio-Pd NPs/CDW mass ratio=6/4, after 24 h catalytic degradation time, at pH=9.0, at 25°C, respectively. Finally, the combination of a simple, easy operation preparation process, excellent performance and cost effective, makes this Bio-Pd NPs with *Shewanella oneidensis* MR-1 bacteria bio-electrochemical cell catalysts a promising option during catalytic degradation process in pharmaceutical industry wastewater treatment.

**Key words:** anova statistical analysis; antibiotics; bio-electrochemical cell; biogenic palladium nanoparticles (bio-pd nps); catalytic removal; coronavirus disease-2019 (covid-19); cost analysis

## 1.Introduction

Emerging contaminants (ECs), sometimes known as contaminants of emerging concern (CECs) can refer to a wide variety of artificial or naturally occurring chemicals or materials that are harmful to human health after long-term disclosure. ECs can be classified into several classes, including agricultural contaminants (pesticides and fertilizers), medicines and antidote drugs, industrial and consumer waste products, and personal care and household cleaning products (Idham et al., 2017; Idham et al., 2021). Antibiotics are one of the ECs that have raised concerns in the previous two decades because they have been routinely and widely used in human and animal health care, resulting in widespread antibiotic residues discharged in surface, groundwater, and wastewater.

Antibiotics, which are widely utilized in medicine, poultry farming and food processing (Arenas and Melo, 2018; Pellerito et al., 2018), have attracted considerable attention due to their abuse and their harmful effects on human health and the ecological environment (Fridkin et al., 2014; Tamma et al., 2017). The misuse of antibiotics induces Deoxyribonucleic Acid (DNA) contamination and accelerates the generation of drug-resistant bacteria and super-bacteria (Huo, 2010; Ferri et al., 2017; Tan et al., 2018); thus, some diseases are more difficult to cure (Tong et al., 2018). A number of studies have revealed that the level of antibiotics in the soil, air and surface water, and even in potable water, is excessive in many areas (Alygizakis et al., 2016; Casanova and Sobsey, 2016; Zhang et al., 2016), which will ultimately accumulate in the human body via drinking water and then damage the body's nervous system, kidneys and blood system. Therefore, it is necessary to develop an efficient method to remove antibiotics present in pharmaceutical industry wastewater.

The uncontrolled, ever-growing accumulation of antibiotics and their residues in the environment is an acute modern problem. Their presence in water and soil is a potential hazard to the environment, humans, and other living beings. Many therapeutic agents are not completely metabolized, which leads to the penetration of active drug molecules into the biological environment, the emergence of new contamination sources, the wide spread of bacteria and microorganisms with multidrug resistance (Jiménez-Tototzintle et al., 2018; Kerrigan, et al., 2018; McConnell et al., 2018). Modern pharmaceutical wastewater facilities do not allow efficient removal of antibiotic residues from the environment (Karthikeyan and Meyer, 2006; Dinh et al., 2017), which leads to their accumulation in ecological systems (Dong et al., 2016; Siedlewicz et al., 2018). Global studies of river pollution with antibiotics have shown that 65% of surveyed rivers in 72 countries on 6 continents are contaminated with antibiotics (Barry, 2019). According to the World Health Organization (WHO), surface and groundwater, as well as partially treated water, containing antibiotics residue and other pharmaceuticals, typically at < 100 ng/l concentrations, whereas treated water has < 50 ng/l concentrations, respectively (Maycock and Watts, 2011). However, the discovery of ECs in numerous natural freshwater sources worldwide is growing yearly. Several antibiotic residues have been reported to have been traced at concentrations greater than their ecotoxicity endpoints in the marine environment, specifically in Europe and Africa (Fekadu et al., 2019). Thus, the European Union's Water Framework Directive enumerated certain antibiotics as priority contaminants (Wang et al., 2017a; Wang et al., 2017b; Wang et al., 2017c). In some rivers, the concentrations were so high that they posed a real danger to both the ecosystem and human health. This matter, the development of effective approaches to the removal of antibiotics from the aquatic environment is of great importance.

The removal of antibiotics and their residues from water and wastewater prior to their final release into the environment is of particular concern (Yang et al., 2021). Modern purification methods can be roughly divided

into the following three categories depending on the purification mechanism: biological treatment (Akyon et al., 2019; Zhang et al., 2019), chemical degradation (de Souza Santos et al., 2015; Yang et al., 2021), and physical removal. Each of these methods has its own advantages and disadvantages. For example, biological purification can remove most antibiotic residues, but the introduction of active organisms into the aquatic environment can upset the ecological balance. Various chemical approaches (ozonation, chlorination, and Fenton oxidation) cannot provide complete purification and, in some cases, lead to the death of beneficial microorganisms due to low selectivity. Photocatalysis is widely used in new environmental control strategies (Zhong et al., 2018; Alagha et al., 2021; Yang et al., 2022). However, this method has a number of key disadvantages, such as insufficient use of visible light, rapid annihilation of photogenerated carriers, and incomplete mineralization, which greatly limits its application (Yang et al., 2021).

Common techniques for the removal of antibiotics are adsorption, membrane filtration, and advanced oxidation processes (AOP) (Abtahi et al., 2018; de Andrade et al., 2018; Pandey et al., 2020). Adsorption and membrane filtration are only temporary solutions in which, the micropollutants are transferred away from the wastewater rather than being treated (degradation in metabolites), while the wastestream also contains a high ionic load (cations and anions) (Bobu et al., 2013; Yagub et al., 2014). The disadvantages of AOP are the high energy consumption and costs, as well as the production of secondary toxic wastestreams (Abtahi et al., 2018; Anjali and Shanthakumar, 2019). An environmentally friendly and highly efficient method that does not produce toxic and high concentrated wastestreams alongside the removal of antibiotics.

Ofloxacin (OFX) is a quinolone antibiotic useful for the treatment of a number of bacterial infections (The American Society of Health-System Pharmacists, 2016). A quinolone antibiotic is a member of a large group of broad-spectrum bacteriocidals that share a bicyclic core structure related to the substance 4-quinolone (Andriole, 1989). They are used in human and veterinary medicine to treat bacterial infections, as well as in animal husbandry, specifically poultry production (Johnson et al., 2003). OFX is well-known for their antimicrobial and anti-inflammatory capabilities (Kritas et al., 2020). OFX is used to treat pneumonia, skin and urinary tract infections (Amini et al., 2020). Severe acute respiratory syndrome (SARS)-CoV-2 (COVID-19) pandemic, which has killed and infected people in 216 countries/territories, has become the most significant pandemic of the century (Sen Gupta et al., 2020). OFX combined with other drugs, has been widely used to minimise COVID-19-induced inflammation in 2020 (Sen Gupta et al., 2020). OFX is a typical fluoroquinolone antibiotic administered to both humans and animals, and after administration, approximately 78% of OFX is excreted (Tong et al., 2011). OFX pharmaceutical compounds enter water resources in various ways, such as human and animal excretions and inefficient industrial wastewater treatment (Amini et al., 2020). In the class of antibiotics, OFX is also recognised as highly refractory and persistent in aquatic water systems. As the biodegradation of OFX is difficult, sewage treatment plants (STPs) have a low removal rate, and the OFX concentrations in the STP effluents of Beijing, Hangzhou, and Vancouver have been determined to be between  $6 \times 10^{-7}$  and  $1.405 \times 10^{-3}$  mg/l (Xiao et al., 2008; Tong et al., 2011).

Doxycycline (DOX), a tetracycline antibiotic, combined with other drugs, has been widely used to minimise *Coronavirus Disease-2019* (COVID-19) induced inflammation in 2020 (Sen Gupta et al., 2020). So, of a sudden, the demand and production of DOX have increased many folds. Due to the high consumptions, there are many chances that DOX will come in effluent treatment through the urinal of COVID-19 patients.

DOX will also come in pharmaceutical industries wastewater, which are producing DOX. These compounds can enter water resources through various channels, including human waste and inefficient industrial wastewater treatment (Amini et al., 2020). DOX is also used to treat chest, skin, and dental infections. DOX pharmaceutical compounds enter water resources in various ways, such as human and animal excretions and inefficient industrial wastewater treatment (Amini et al., 2020). They also enter the environment due to the improper disposal of expired pharmaceuticals in the garbage or sewage system. The traditional methods for treating such wastewater like coagulation, flocculation, or precipitation lacks efficiency and cannot remove them completely (Adams et al., 2002; Stackelberg et al., 2007; Garg et al., 2016). On the other hand, biological treatments are time-consuming and produce a large quantity of sludge that cannot be used further (Bansal et al., 2016). However, most of these technologies have been reported to have drawbacks such as low efficiency, secondary pollution, and high capital costs. As a result, it is necessary to develop practical technologies based on modern world engineering science to find a better and more cost-effective solution to treat water and wastewater for human consumption. In recent years, advanced oxidation processes (AOPs) have piqued the interest of many researchers due to their potential application in the efficient mineralisation of refractory substances (Rezaei et al., 2019), more effective and sustainable in the long term (Wei et al., 2020; Babaei et al., 2021).

Palladium (Pd) is a precious metal and is one of the most important elements in chemical catalysis, (Xu et al., 2019) electronic circuits, jewelry, semiconductors, ornaments, corrosion-resistant equipment and thermocouples (Folens et al., 2016). With the increasing use of palladium in the past 30 years, a substantial amount of waste Pd is discharged into the environment, which results in the presence of higher levels of Pd in road dust, airborne particulates, groundwater tables and soil. Moreover, the chemical catalysis and electroplating industries generate a large amount of wastewater containing palladium. In epidemiological studies, exposure to Pd has been verified to cause not only acute toxicity, hypersensitivity with respiratory symptoms, and urticaria, but also some immune system diseases, indicating it is a significant hazard to human health because Pd ions are one of the most significant metal sensitizers. Thus, the recovery and reuse of this metal, based on the notion of recycling waste, (Sattayarut et al., 2019) are necessary to recover this valuable material and to treat wastewater to promote green chemistry, economic efficiency and sustainability (Noah et al., 2016).

Under suitable conditions, Pd adsorbs more than 900 times its volume of hydrogen (H<sub>2</sub>) (Dekura et al., 2019). This metal is an essential catalyst for energy conversion, chemical reaction, and abiotic electrochemical processes (Guo et al., 2013; Wu et al., 2018). The Pd is frequently applied in different methods due to its catalytic activity; therefore, it is often used as a catalyst in its NPs size (Coy et al., 2020). Smaller sizes allow a monodisperse distribution of the particles and provide a high surface area that increases the catalytic activity (Saldan et al., 2015). The NPs can be chemically/electrochemically or biologically produced (De Windt et al., 2006; Saldan et al., 2015; Wu et al., 2018). Chemical synthesis of Pd NPs requires the use of a series of toxic and expensive agents, whereas strong reductants and stabilisers are required to reduce the metals to zero-valent and as carrier materials (De Corte et al., 2012). Electrodeposition of Pd is also used and is obtained by using an underpotential deposition condition, e.g. potentials higher than the Nerst one (Previdello et al., 2017; Espino-López et al., 2018). Biological synthesis is less harmful to the environment than chemical production as no secondary toxic wastestream is produced (Hennebel et al., 2009a; Hennebel et al., 2009b).

Production of biogenic palladium nanoparticles (bio-Pd NPs) occurs through microorganisms or plants, where they are responsible for the conversion of Pd<sup>+2</sup> to Pd<sup>0</sup> (Yong et al., 2002; De Windt et al., 2005; Sathishkumar et al., 2009; Sahin and Gubbuk, 2022). Different microorganisms and plants have been used through extensive research to obtain a higher functionality (Courtney et al., 2016; Tuo et al., 2017;

Xiong et al., 2018). When biological carriers are used for the production of bio-Pd NPs, all Pd<sup>+2</sup> that is taken up inside or on the biological carrier will be converted to Pd<sup>0</sup> (Xu et al., 2018; Sahin and Gubbuk, 2022). No difference in terminology is made for bio-Pd NPs inside or outside the cells when production occurs through microorganisms. While the production pathway of most of the microorganisms remains unknown, it was recently unravelled for *Shewanella oneidensis* MR-1. *Shewanella oneidensis* is a facultative bacterium (Venkateswaran et al., 1999) and the special interest in *Shewanella oneidensis* MR-1 revolves around its behavior in an anaerobic environment contaminated by heavy metals such as iron (Fe), lead (Pb) and uranium (U). Experiments suggest it may reduce ionic mercury (Hg) to elemental Hg, (Wiatrowski et al., 2006), and ionic silver (Ag) to elemental Ag (Ng et al., 2013a; Ng et al., 2013b). Cellular respiration for *Shewanella oneidensis* MR-1 is not restricted to heavy metals though; can also target sulfates (SO<sub>4</sub><sup>2-</sup>), nitrates (NO<sub>3</sub><sup>-</sup>) and chromates (CrO<sub>4</sub><sup>2-</sup>) when grown anaerobically. *Shewanella oneidensis* MR-1 was shown that nicotinamide adenine dinucleotide (NAD<sup>+</sup>) + hydrogen (H) (NADH) dehydrogenase and hydrogenase enzymes played an important role in the production of bio-Pd NPs, when converting all Pd<sup>+2</sup> present in the cell to Pd<sup>0</sup> (Fredrickson et al., 2008; Deplanche et al., 2010; Hou et al., 2017; Yang et al., 2020). It was found that *Escherichia coli* was still viable after exposure to Pd, and hence metabolically active but not culturable (Joudeh et al., 2021). For plants, the biomolecules are responsible for the production, e.g., polyols, proteins, flavones, flavonoids, and tannins (Qazi et al., 2016; Sarmah et al., 2019). Besides these carriers, the potential use of anaerobic granular sludge for production was recently discovered (Suja et al., 2014; Quan et al., 2020). Other than using different biological carriers, the performance of bio-Pd NPs can be tuned through modification in production methods. One of the commonly used techniques is the formation of bimetallic NPs; Pd has been combined with other metals of interest, e.g., gold (Au), silver (Ag), iron (Fe), and ruthenium (Ru) (De Corte et al., 2011; Omajali et al., 2019; Sivamaruthi et al., 2019).

The use of bio-Pd NPs for the removal of pharmaceutical compounds has been tested with promising results (Forrez et al., 2011; Wang et al., 2018). However, the application of bio-Pd NPs for the removal of fluorinated pharmaceutical compounds (e.g., ciprofloxacin, citalopram, and atorvastatin), which are highly used and for which removal efficiencies tend to be low, have not been well studied yet (Forrez et al., 2011; Miao et al., 2018; Osawa et al., 2019; Antonelli et al., 2020). Martins et al. (2017) assessed the removal of several antibiotics by bio-Pd NPs, but no removal of fluorinated antibiotics as a result of the catalytic activity of the NPs was detected. The study was carried out in a synthetic medium, where the matrix composition is fairly simple in contrast to real environmental matrices. Nevertheless, a removal of 87.7% of ciprofloxacin was found after 25 hr and at pH = 3.2 with 30 mg of Pd in the form of bio-Pd NPs (He et al., 2020). The disadvantage of this method is the low pH and high concentrations of Pd needed. Moreover, the degradation of persistent fluorinated antibiotics, other than ciprofloxacin, with bio-Pd NPs required further study, especially in environmentally relevant matrices. Ideally, effective removal is accomplished with the use of a lower concentration of Pd, shorter reaction time, higher pH, and in environmentally relevant concentrations are required.

The produced bio-Pd NPs are widely utilised to remediate micropollutants in the environment (e.g., pharmaceuticals and antimicrobial agents) (De Corte et al., 2012; Hoffmann, 2012; Hazarika et al., 2017). Several “hard to degrade” micropollutants such as diatrizoate, trichloroethylene, diclofenac, chromate, chlorophenols, and lindane have been efficiently transformed by bio-Pd NPs (De Gussemme et al., 2011; De Corte et al., 2012; Quan et al., 2019). Microbial degradation often stalls or slows down at micropollutant relevant concentration range due to mass transfer limitation across the cell membrane (Verlicchi et al., 2010; Ehrl et al., 2019; Kundu et al., 2019). Some of the micropollutants are even resistant to microbial enzymes; nevertheless, enzymatic removal of micropollutants can also produce toxic by-products which is not desired

(Feng et al., 2021). Therefore, oxidative techniques are often used; however, dangerous explosive compounds are needed (Silva et al., 2017). Hence, developing alternative sustainable approaches is of utmost importance. The bio-Pd NPs hold promise to overcome the hurdle of micropollutants removal in a sustainable way (1) reusable, (2) bio origin, environment-friendly production, and (3) high catalytic activity.

A more recent application of bio-Pd NPs can be found in electrochemical systems. The bio-Pd NPs are coated on anodes and used to increase electricity generation in a microbial electrochemical fuel cell (MFC) (Orozco et al., 2010). The bio-Pd NPs can also be fixed on electrodes to increase the electroconductivity of the electrochemical cell. The electro-active bacteria used for the bio-Pd production and Pd will increase the electro-conductivity. This improved electro-conductivity results in an increased electron transfer and thus a higher catalytic activity (Quan et al., 2015a; Quan et al., 2015b; Cheng et al., 2017). Some recent reviews have mainly underlined the potential use of green synthesis for metal NP production with their advantages and general applications (Kumari et al., 2019; Fahmy et al., 2020; Singh et al., 2020). However, the overview of the mechanisms and optimisation of production methods specific for bio-Pd NPs with their novel applications such as in electrochemical systems are missing. A summary of different methods specific to how to increase the catalytic activity of the produced bio-Pd NPs is also present. There is a clear need to acquire a better understanding of the role of bio-Pd NPs in electrochemical cells as the pathway of the microbial production.

In this study, biogenic-palladium nanoparticles (bio-Pd NPs) with *Shewanella oneidensis* MR-1 bacteria as a heterostructure bio-

electrochemical cell catalys was examined during catalytic degradation process in the efficient removal of Ofloxacin (OFX) and Doxycycline (DOX) micropollutants from pharmaceutical industry wastewater plant, İzmir, Turkey. Different pH values (3.0, 4.0, 6.0, 7.0, 9.0 and 11.0), increasing micropollutants (OFX and DOX) concentrations (5 mg/l, 15 mg/l, 30 mg/l and 45 mg/l), increasing Bio-Pd NPs concentrations (5 mg/l, 10 mg/l, 20 mg/l, 30 mg/l, 40 mg/l and 60 mg/l), different Bio-Pd NPs/cell dry weight (CDW) mass ratios (5/5, 6/4, 7/3, 8/2, 9/1, 1/9, 2/8, 3/7 and 4/6), increasing recycle times (1., 2., 3., 4., 5., 6. and 7.) was operated during catalytic degradation process in the efficient removals of OFX and DOX micropollutants in pharmaceutical industry wastewater. The characteristics of the synthesized NPs were assessed using DRS, EDX, FESEM, FTIR, ICP-MS, TEM, XRD and XPS analyses, respectively. The catalytic degradation mechanisms of bio-Pd NPs with *Shewanella oneidensis* MR-1 bacteria as a heterostructure bio-electrochemical cell catalysts and the reaction kinetics of OFX and DOX micropollutants were evaluated in pharmaceutical industry wastewater during catalytic degradation process. ANOVA statistical analysis was used for all experimental samples.

## 2. Materials and Methods

### 2.1. Characterization of Pharmaceutical Industry Wastewater

Characterization of the biological aerobic activated sludge proses from a pharmaceutical industry wastewater plant, İzmir, Turkey was performed. The results are given as the mean value of triplicate samplings (Table 1).

Parameters	Unit	Concentrations
Chemical oxygen demand-total (COD <sub>total</sub> )	(mg/l)	4000
Chemical oxygen demand-dissolved (COD <sub>dissolved</sub> )	(mg/l)	3200
Biological oxygen demand-5 days (BOD <sub>5</sub> )	(mg/l)	1500
BOD <sub>5</sub> / COD <sub>dissolved</sub>		0.5
Total organic carbons (TOC)	(mg/l)	1800
Dissolved organic carbons (DOC)	(mg/l)	1100
pH		8.3
Salinity as Electrical conductivity (EC)	(mS/cm)	1552
Total alkalinity as CaCO <sub>3</sub>	(mg/l)	750
Total volatile acids (TVA)	(mg/l)	380
Turbidity ( <i>Nephelometric Turbidity unit, NTU</i> )	NTU	7.2
Color	1/m	50
Total suspended solids (TSS)	(mg/l)	250
Volatile suspended solids (VSS)	(mg/l)	187
Total dissolved solids (TDS)	(mg/l)	825
Nitride (NO <sub>2</sub> <sup>-</sup> )	(mg/l)	1.7
Nitrate (NO <sub>3</sub> <sup>-</sup> )	(mg/l)	1.91
Ammonium (NH <sub>4</sub> <sup>+</sup> )	(mg/l)	2.3
Total Nitrogen (Total-N)	(mg/l)	3.2
SO <sub>3</sub> <sup>2-</sup>	(mg/l)	21.4
SO <sub>4</sub> <sup>2-</sup>	(mg/l)	29.3
Chloride (Cl <sup>-</sup> )	(mg/l)	37.4
Bicarbonate (HCO <sub>3</sub> <sup>-</sup> )	(mg/l)	161
Phosphate (PO <sub>4</sub> <sup>3-</sup> )	(mg/l)	16
Total Phosphorus (Total-P)	(mg/l)	40
Total Phenols	(mg/l)	70
Oil & Grease	(mg/l)	220
Cobalt (Co <sup>+3</sup> )	(mg/l)	0.2
Lead (Pb <sup>+2</sup> )	(mg/l)	0.4
Potassium (K <sup>+</sup> )	(mg/l)	17
Iron (Fe <sup>+2</sup> )	(mg/l)	0.42
Chromium (Cr <sup>+2</sup> )	(mg/l)	0.44
Mercury (Hg <sup>+2</sup> )	(mg/l)	0.35
Zinc (Zn <sup>+2</sup> )	(mg/l)	0.11

**Table 1:** Characterization of Pharmaceutical Industry Wastewater

## 2.2. Experimental Chemicals

The M9 medium used for washing the bio-Pd NPs was prepared based on the recipe and  $\text{Na}_2\text{HPO}_4$ ,  $\text{NaCl}$ ,  $\text{KH}_2\text{PO}_4$  and  $\text{NH}_4\text{Cl}$  purchased from Merck (Merck, Germany). The KOH tablets used as electrolyte was purchased from Merck (Merck, Germany). For Inductively coupled plasma mass spectrometry (ICP-MS) analysis, ultra-pure water (Resistivity > 18.2 M $\Omega$  cm, Millipore, France) was used. The  $\text{Na}_2\text{PdCl}_4$  powder (98%), phosphate-buffered saline (PBS) tablets, LB broth used for bio-Pd NPs production, and methyl orange for the activity test were purchased from Sigma-Aldrich (Sigma-Aldrich, Germany). Pro analysis purity level 14 mol/l  $\text{HNO}_3$  (Sigma-Aldrich, Germany), further purified by sub-boiling distillation, and 9.8 mol/l  $\text{H}_2\text{O}_2$  (Sigma-Aldrich, Germany) were used for acid digestion. 1 g/l single-element standard solutions of Pd and Rh (Merck, Germany) were used for method development and calibration purposes, and for internal standardization, respectively.

## 2.3. Preparation of Biogenic Palladium Nanoparticles (Bio-Pd NPs) Solution

The production of bio-Pd NPs was carried out as described by De Windt et al. (2005). *Shewanella oneidensis* MR-1 cells were grown in LB medium overnight at 28°C on a shaker, and harvested by centrifuging at 10000 rpm for 10 min. The cells were washed three times with M9 medium and resuspended in M9 medium to a final optical of  $\text{OD}_{610} = 0.5$  with Spectronic 200 (Thermofischer, USA). The  $\text{Na}_2\text{PdCl}_4$  was added to the resuspended solution at a concentration of 50 mg/l  $\text{Pd}^{+2}$  and this solution was incubated overnight on a shaker at 20°C. Production of different types of bio-Pd NPs was performed in a custom-built experimental setup. Corresponding controls were prepared in the same manner but were not exposed to  $\text{H}_2(\text{g})$ . The bio-Pd NPs produced and controls were washed three times with PBS and stored at 5°C.

## 2.4. Synthesis of the biogenic palladium nanoparticles under anaerobic conditions

1 gram wet cells was added to 200 ml of  $\text{PdCl}_2$  solution (200 mg/l), the pH of the solution was adjusted to 2.0, and the container was then sealed. The solutions were incubated under anaerobic conditions by flushing with  $\text{N}_2(\text{g})$  for 5 min. After incubation at 30°C for 60 min to allow for  $\text{Pd}^{+2}$  biosorption, the bio-Pd NPs was harvested and collected by centrifugation (8000 rpm, 8 min) and resuspended in deionized water. The Bio-Pd(II) was transferred to a 100 ml three-necked flask. Then, the three-necked flask was flushed with  $\text{H}_2(\text{g})$  and left at 25°C with stirring (150 rpm) in  $\text{H}_2(\text{g})$  atmosphere. After 5 h, the bio-Pd NPs used in the next experiment was collected by centrifugation (8000 rpm, 8 min) and washed twice with deionized water. 50 ml  $\text{PdCl}_2$  solution at pH=2.0 was added to a 100 ml round-bottomed flask. 100 ml round-bottomed flask was flushed with  $\text{H}_2(\text{g})$ , and left at 25°C with stirring (150 rpm) in  $\text{H}_2(\text{g})$  atmosphere, collected by centrifugation (8000 rpm, 8 min) and washed twice with deionized water after 5 h to preparation Pd(0) without *Shewanella oneidensis* MR-1.

## 2.5. Experimental Conditions for bio-Pd NPs production

An experimental reactor setup (in triplicate) containing an electrochemical cell (EC) connected to a glass column was used to produce bioPd NPs. A two-compartment EC (dimensions: 25 cm x 10.0 x 3.0 cm) made from two Perspex® frames was used to separate the cation exchange membrane (CEM) (Membrane International Inc., USA) from the electrodes. A stainless-steel electrode was used as the cathode (dimensions: 5 x 20 cm) and an iridium (Ir) electrode was used as the anode. Between the compartments and CEM, rubber sheets were placed to create a liquid-tight seal, and the frames were bolstered. A pump at 255 ml/min flow rate was used to recirculate the KOH electrolyte. The current of the EC was controlled by a power supply, Faraday's Law was used to calculate the amount of  $\text{H}_2(\text{g})$  produced based on the current applied. The EC was connected to a glass column (wrapped in aluminum foil to prevent

light penetration), in which the microorganisms/ $\text{Pd}^{+2}$  solution was transferred in, after incubation. The top of the glass column was connected to a gascounter. The bottom of the column contained a two-way connector between the EC and a gasbag for  $\text{N}_2(\text{g})$  flushing, both regulated by a valve.

## 2.6. Characterization of the bio-Pd NPs

### 2.6.1. Transmission Electron Microscopy (TEM) Analysis

The obtained bio-Pd NPs was collected and harvested by centrifugation (8000 rpm, 5 min), washed twice with deionized water, and resuspended in ethanol ( $\text{C}_2\text{H}_6\text{O}$ ) and dripped onto a carbon-coated copper (Cu) *Transmission Electron Microscopy* (TEM) grid. Vacuum drying then occurred to the biological Pd(0) for 24 h at 25°C room temperature. The dry samples on the Cu grid were viewed and examined by TEM Analysis recorded in a JEOL JEM 2100F, Japan under 200 kV accelerating voltage. The size and structure of the bio-Pd NPs samples were identified with TEM analysis.

### 2.6.2. Field Emission Scanning Electron Microscopy (FESEM) and Energy Dispersive X-Ray (EDX) Spectroscopy Analysis

The morphological features and structure of the bio-Pd NPs was determined by Field Emission Scanning Electron Microscopy (FESEM) (FESEM, Hitachi S-4700). The elements on the surface of the bio-Pd NPs were analysed using energy dispersive X-ray analysis (EDX) with EDX spectrometry device (TESCAN Co., Model III MIRA). The biological Pd NPs on *Shewanella oneidensis* MR-1 were harvested and collected by centrifugation (8000 rpm, 5 min), resuspended in  $\text{C}_2\text{H}_6\text{O}$  and dripped onto a thin film. The samples of the biological Pd NPs on *Shewanella oneidensis* MR-1 were dried overnight in a vacuum drying oven at 30°C and analysed by FESEM and EDX.

### 2.6.3. X-Ray Diffraction (XRD) Analysis

Powder XRD patterns were recorded on a Shimadzu XRD-7000, Japan diffractometer using Cu  $\text{K}\alpha$  radiation ( $\lambda = 1.5418 \text{ \AA}$ , 40 kV, 40 mA) at a scanning speed of 1°/min in the 10-80° 2 $\theta$  range. Raman spectrum was collected with a Horiba Jobin Yvon-Labram HR UV-Visible NIR (200-1600 nm) Raman microscope spectrometer, using a laser with the wavelength of 512 nm. The spectrum was collected from 10 scans at a resolution of 2 /cm. The zeta potential was measured with a SurPASS Electrokinetic Analyzer (Austria) with a clamping cell at 300 mbar.

### 2.6.4. X-Ray Photoelectron Spectroscopy (XPS) Analysis

The valence state of the biogenic palladium nanoparticles was investigated and was analyzed using XPS (ESCALAB 250Xi, England). XPS used an Al  $\text{K}\alpha$  source and surface chemical composition and reduction state analyses was done, with the core levels recorded using a pass energy of 30 eV (resolution approximately 0.10 eV). The peak fitting of the individual core-levels was done using XPS-peak 41 software, achieving better fitting and component identification. All binding energies were calibrated to the C 1s peak originating from C-H or C-C groups at 284.6 eV.

### 2.6.5. Inductively Coupled Plasma Mass Spectrometry (ICP-MS) Analysis

Bulk ICP-MS, Agilent 8800 ICP-MS instrument (Agilent Technologies, Japan), analysis was performed to determine the concentration of Pd in the different bio-Pd NPs samples. For bulk analysis, the bio-Pd NPs samples were acid digested in closed Savillex® PFA beakers prior to ICP-MS. 5 ml of suspended bio-Pd in PBS was centrifuged at 10000 xg for 30 min, after which the supernatant was removed. The resulting pellet was acid digested with 1.5 ml of 14 mol/l  $\text{HNO}_3$  and 0.5 ml of 9.8 mol/l  $\text{H}_2\text{O}_2$ . The closed beakers were heated to 115°C overnight on a hot plate. After complete mineralization, the digestates were evaporated at 90°C until

dryness, then redissolved in 2.0 ml of 0.35 mol/l HNO<sub>3</sub>. This solution was further diluted with 0.35 mol/l HNO<sub>3</sub> and rhodium (Rh) was added as the internal standard (final concentration = 2 µg/l) to compensate for potential matrix effects and/or signal instability.

#### 2.6.6. Fourier Transform Infrared Spectroscopy (FTIR) Analysis

The FTIR spectra of experimental samples was recorded using the FT-NIR spectroscope (RAYLEIGH, WQF-510).

#### 2.6.7. Diffuse Reflectance UV-Vis Spectra (DRS) Analysis

DRS Analysis in the range of 200–800 nm were recorded on a Cary 5000 UV-Vis Spectrophotometer from Varian. DRS was used to monitor the OFX and DOX concentrations in experimental samples.

#### 2.7. OFX Removal Using Biological Pd NPs on *Shewanella oneidensis* MR-1 cells

A certain amount of OFX was dissolved in ultrapure water acidified with glacial acetic acid (CH<sub>3</sub>COOH) (5 ml/l), and the solution was adjusted to pH=3.2 with hydrochloric acid (HCl) (1 mol/l). 30 mg biological Pd NPs was resuspended in 20 ml of this OFX solution. Catalytic removal of OFX using this biological Pd NPs was carried out in the dark at 25°C with stirring at 150 rpm. 3 ml of the reaction mixture was removed every 5 h with a syringe and passed through a syringe filter with a pore size of 0.22 µm to remove biological Pd(II) or biological Pd(0). An ultraviolet (UV) spectrophotometer was used to detect the residual content of OFX in the supernatant at 420 nm, and the removal of OFX was calculated by comparison with a standard curve. When the removal of OFX was conducted under anaerobic conditions, 30 mg biological Pd NPs was transferred into the OFX solution, and then H<sub>2</sub>(g) was bubbled into the suspension for at least 10 min from the bag, and a hose was used to connect a balloon of H<sub>2</sub>(g) and the reactor vessel.

#### 2.8. DOX Removal Using Biological Pd NPs on *Shewanella oneidensis* MR-1 cells

A certain amount of DOX was dissolved in ultrapure water acidified with CH<sub>3</sub>COOH (5 ml/l), and the solution was adjusted to pH=3.2 with HCl (1 mol/l). 30 mg biological Pd NPs was resuspended in 20 ml of this DOX solution. Catalytic removal of DOX using this biological Pd NPs was carried out in the dark at 25°C with stirring at 150 rpm. 3 ml of the reaction mixture was removed every 5 h with a syringe and passed through a syringe filter with a pore size of 0.22 µm to remove biological Pd(II) or biological Pd(0). An ultraviolet (UV) spectrophotometer was used to detect the residual content of DOX in the supernatant at 240 nm, and the removal of DOX was calculated by comparison with a standard curve. When the removal of DOX was conducted under anaerobic conditions, 30 mg biological Pd NPs was transferred into the DOX solution, and then H<sub>2</sub>(g) was bubbled into the suspension for at least 10 min from the bag, and a hose was used to connect a balloon of H<sub>2</sub>(g) and the reactor vessel.

#### 2.9. Catalytic Activity Test

The catalytic activity of bio-Pd NPs was evaluated by the removal of 100 mg/l Methyl Orange (in biological triplicates), in serum flasks. Suspended bio-Pd was centrifuged at 10000 x g for 10 min, and the pellet of centrifuged bio-Pd corresponded to 80.95 µg Pd. The pellet was resuspended in 19.2 ml deionized water and 0.8 ml Methyl Orange stock solution (7.63 mmol/l) was added. The serum flasks were flushed with 100% N<sub>2</sub>(g) for 20 cycles, subsequently, 120 ml of 100% H<sub>2</sub>(g) was added. 1 ml sample was taken at 0 min, 10 min, 20 min, 40 min, 60 min, 80 min, 100 min and 120 min and was filtered using a 0.20 µm filter. The absorbance was measured at a λ<sub>max</sub> = 465 nm using a Cary 5000 UV-Vis Spectrophotometer from Varian. Deionized water and (filtered) suspended bio-Pd in deionized water were used as a control for the absorbance measurements. Suspended microorganisms without Pd were used as a control for the catalytic activity test.

#### 2.10. Analytical Procedures

Chemical oxygen demand-total (COD<sub>total</sub>), chemical oxygen demand-dissolved (COD<sub>dissolved</sub>), total phosphorus (Total-P), phosphate phosphorus (PO<sub>4</sub><sup>3-</sup>-P), total nitrogen (Total-N), ammonium nitrogen (NH<sub>4</sub><sup>+</sup>-N), nitrate nitrogen (NO<sub>3</sub><sup>-</sup>-N), nitrite nitrogen (NO<sub>2</sub><sup>-</sup>-N), biological oxygen demand 5-days (BOD<sub>5</sub>), pH, Temperature [(°C)], total suspended solids (TSS), total volatile suspended solids (TVSS), total organic carbon (TOC), Oil, Chloride (Cl<sup>-</sup>), total phenol, total volatile acids (TVA), dissolved organic carbon (DOC), total alkalinity, turbidity, total dissolved solid (TDS), color, sulfide (SO<sub>3</sub><sup>2-</sup>), sulfate (SO<sub>4</sub><sup>2-</sup>), bicarbonate (HCO<sub>3</sub><sup>-</sup>), salinity, cobalt (Co<sup>3+</sup>), lead (Pb<sup>2+</sup>), potassium (K<sup>+</sup>), iron (Fe<sup>2+</sup>), chromium (Cr<sup>2+</sup>), Mercury (Hg<sup>2+</sup>) and zinc (Zn<sup>2+</sup>) were measured according to the Standard Methods (2017) 5220B, 5220D, 4500-P, 4500-PO<sub>4</sub><sup>3-</sup>, 4500-N, 4500-NH<sub>4</sub><sup>+</sup>, 4500-NO<sub>3</sub><sup>-</sup>, 4500-NO<sub>2</sub><sup>-</sup>, 5210B, 4500-H<sup>+</sup>, 2320, 2540D, 2540E, 5310, 5520, 4500-Cl<sup>-</sup>, 5530, 5560B, 5310B, 2320, 2130, 2540E, 2120, 4500-SO<sub>3</sub><sup>2-</sup>, 4500-SO<sub>4</sub><sup>2-</sup>, 5320, 2520, 3500-Co<sup>3+</sup>, 3500-Pb<sup>2+</sup>, 3500-K<sup>+</sup>, 3500-Fe<sup>2+</sup>, 3500-Cr<sup>2+</sup>, 3500-Hg<sup>2+</sup>, 3500-Zn<sup>2+</sup>, respectively (Baird et al., 2017).

Total-N, NH<sub>4</sub><sup>+</sup>-N, NO<sub>3</sub><sup>-</sup>-N, NO<sub>2</sub><sup>-</sup>-N, Total-P, PO<sub>4</sub><sup>3-</sup>-P, total phenol, Co<sup>3+</sup>, Pb<sup>2+</sup>, K<sup>+</sup>, Fe<sup>2+</sup>, Cr<sup>2+</sup>, Hg<sup>2+</sup>, Zn<sup>2+</sup>, SO<sub>3</sub><sup>2-</sup>, and SO<sub>4</sub><sup>2-</sup> were measured with cell test spectroquant kits (Merck, Germany) at a spectroquant NOVA 60 (Merck, Germany) spectrophotometer (2003).

The measurement of color was carried out following the methods described by Olthof and Eckenfelder (1976) and Eckenfelder (1989). According these methods, the color content was determined by measuring the absorbance at three wavelengths (445 nm, 540 nm and 660 nm), and taking the sum of the absorbances at these wavelengths. In order to identify the color in pharmaceutical industry wastewater (25 ml) was acidified at pH=2.0 with a few drops of 6 N HCl and extracted three times with 25 ml of ethyl acetate. The pooled organic phases were dehydrated on sodium sulphate, filtered and dried under vacuum. The residue was silylated with bis(trimethylsilyl)trifluoroacetamide (BSTFA) in dimethylformamide and analyzed by gas chromatography–mass spectrometry (GC-MS) and gas chromatograph (GC) (Agilent Technology model 6890N) equipped with a mass selective detector (Agilent 5973 inert MSD). Mass spectra were recorded using a VGTS 250 spectrometer equipped with a capillary SE 52 column (HP5-MS 30 m, 0.25 mm ID, 0.25 µm) at 220°C with an isothermal program for 10 min. The initial oven temperature was kept at 50°C for 1 min, then raised to 220°C at 25°C/min and from 200 to 300°C at 8°C/min, and was then maintained for 5.5 min. High purity He (g) was used as the carrier gas at constant flow mode (1.5 ml/min, 45 cm/s linear velocity).

The total phenol was monitored as follows: 40 ml of pharmaceutical industry wastewater was acidified to pH=2.0 by the addition of concentrated HCl. Total phenol was then extracted with ethyl acetate. The organic phase was concentrated at 40°C to about 1 ml and silylated by the addition of N,O-bis(trimethylsilyl) acetamide (BSA). The resulting trimethylsilyl derivatives were analysed by GC-MS (Hewlett-Packard 6980/HP5973MSD).

Methyl tertiary butyl ether (MTBE) was used to extract oil from the water and NPs. GC-MS analysis was performed on an Agilent gas chromatography (GC) system. Oil concentration was measured using a UV–vis spectroscopy fluorescence spectroscopy and a GC–MS (Hewlett-Packard 6980/HP5973MSD). UV–vis absorbance was measured on a UV–vis spectrophotometer and oil concentration was calculated using a calibration plot which was obtained with known oil concentration samples.

#### 2.11. Statistical Analysis

ANOVA analysis of variance between experimental data was performed to detect F and P values. The ANOVA test was used to test the differences between dependent and independent groups, (Zar, 1984). Comparison between the actual variation of the experimental data averages and standard deviation is expressed in terms of F ratio. F is equal (found

variation of the date averages/expected variation of the date averages). P reports the significance level, and d.f indicates the number of degrees of freedom. Regression analysis was applied to the experimental data in order to determine the regression coefficient  $R^2$ , (Statgraphics Centurion XV, 2005). The aforementioned test was performed using Microsoft Excel Program.

All experiments were carried out three times and the results are given as the means of triplicate samplings. The data relevant to the individual pollutant parameters are given as the mean with standard deviation (SD) values.

### 3. Results And Discussions

#### 3.1. Bio-Electrochemical Cell Mechanism of Bio-Pd NPs Production

Each bacteria is different, bio-Pd NPs synthesis mainly depends on the outer membrane c-type cytochrome and hydrogenase enzyme (De Windt et al., 2005; Fredrickson et al., 2008; Deplanche et al., 2010; De Corte et al., 2012; Hou et al., 2017). The c-type cytochrome is responsible for transporting the electrons across the bacterial cell to the metals (Ng et al., 2013a; Ng et al., 2013b). At the same time, the hydrogenase contains redox proteins that are important for reducing metals and consequently contribute to the formation of metal particles. Here, the  $Pd^{+2}$  will be converted to  $Pd^0$ ; hence, the formed particles can be found on the cell wall, inside the cell membranes, or cytoplasm (Fredrickson et al., 2008; Hennebel et al., 2011; Bucking et al., 2012; Ng et al., 2013a; Ng et al., 2013b; Dundas et al., 2018). The electroactive bacterium, *Shewanella oneidensis* MR-1, is a well-established microorganism for the production of metal NPs. It has the characteristics to perform the biological dissimilatory metal reduction process (DMR). In this biological process, various metal (loid)s, outside the microorganism, are used as a terminal electron acceptor. Energy is conserved by oxidising an (in)organic matter and reducing a metal (Lovley, 1993; Shi et al., 2009; Dundas et al., 2018; Xiong et al., 2018). The mechanism used by the microorganisms depends

on the type of metal used for NP production (Lovley, 1993; Marshall et al., 2006; Mikheenko et al., 2008; Shi et al., 2009; Deplanche et al., 2010). The production process of bio-Pd NPs can be in general described in three steps: (1) biological adsorption (biosorption) on the cell surface, (2) bioreduction of  $Pd^{+2}$  to  $Pd^0$  in- and outside the cell wall, and (3) autocatalytic reduction, of  $Pd^{+2}$  to  $Pd^0$  which is not enzymatic and clusters onto the Pd NPs of the cell wall (De Corte et al., 2012; Deplanche et al., 2014; Xu et al., 2018). The production of bio-Pd NPs by *Shewanella oneidensis* MR-1 will be discussed in detail here, due to the general and beneficial character of the microorganisms for the production of bio-Pd NPs. First, biosorption of  $Pd^{+2}$  on the cell wall can occur by ion exchange, electrostatic interaction, complexation, and physical adsorption which was shown in FTIR analysis by Xu et al. (2018). Independent of the type of biosorption process, the  $Pd^{+2}$  is converted to  $Pd^0$ , by chemical or autocatalytic conversion (De Corte et al., 2012; Ng et al., 2013a; Ng et al., 2013b; Deplanche et al., 2014). When ion exchange, electrostatic interaction, or complexation occurs, the functional groups of the cell surface have an essential role and are responsible for attaching the  $Pd^{+2}$  to the cell wall. Nevertheless, it is also possible to have physical adsorption, where the functional groups do not intervene in attaching the  $Pd^{+2}$  to the cell wall (Xu et al., 2018). However, besides the biosorption, the cell wall can convert the  $Pd^{+2}$  to  $Pd^0$  which was observed in scanning electron microscopic energy-dispersive X-Ray spectroscopy (SEM-EDX) and transmission electron microscopic (TEM) images (Xu et al., 2018). This indicates that bioreduction can be achieved through the hydroxyl group present on the cell surface. Interestingly, Yang et al. (2020) found that this bioreduction of  $Pd^{+2}$  to  $Pd^0$  occurs through the c-type cytochrome on the cell wall, more specific Cym A (such as OmCA and MtrC). Furthermore, the production of bio-Pd NPs inside the cells is also present. Yang et al. (2020), suggested that the NADH-dehydrogenase, [FeFe]-hydrogen (HyaA), and [NiFe]-hydrogenase (HyaB) are essential for the bio-Pd NPs production, as they influence the size, distribution, and the number of bio-Pd NPs (Figure 1).

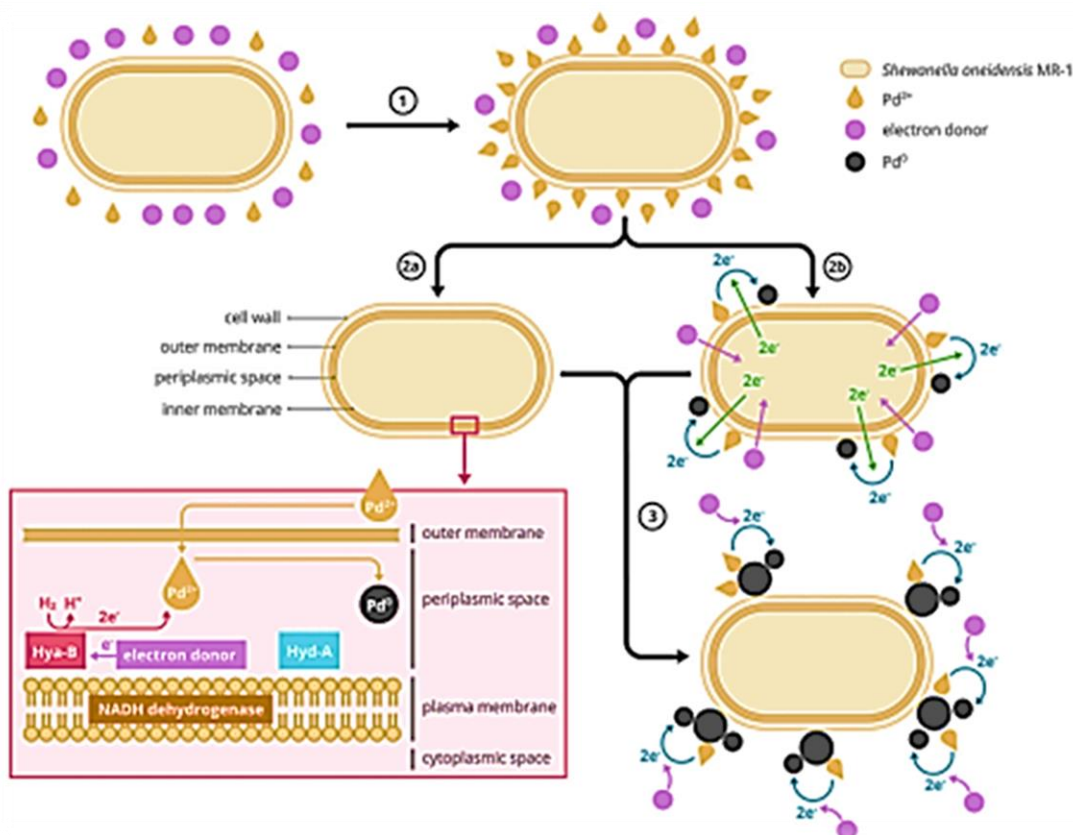


**Figure 1:** Production mechanism of bio-Pd NPs inside and outside the microorganisms: (1) Adsorption of  $\text{Pd}^{2+}$  on the cell wall, (2a) conversion of  $\text{Pd}^{2+}$  to  $\text{Pd}^0$  inside the cell, (2b) on the cell wall, and (3) autocatalytic conversion of  $\text{Pd}^{2+}$  to  $\text{Pd}^0$  outside the cell. The figure was inspired by Deplanche et al. (2010), Ng et al. (2013a), and Yang et al. (2020).

These enzymes are mainly responsible for the formation of bio-Pd NPs inside and outside the cell membrane (Yang et al., 2020). Whereas [NiFe]-hydrogenase produces hydrogen from formate and oxidises hydrogen, [FeFe]-hydrogenase works together with formate dehydrogenases in the form of formate-hydrogen lyase that generates hydrogen from formate (Yang et al., 2020). Dundas et al. (2018), stated that the hydrogenase enzymes play an essential role in facilitating the reduction process of  $\text{Pd}^{2+}$  by *Shewanella oneidensis* MR-1. It was observed that this process followed the pseudo-first-order kinetic model (Ng et al., 2013a; Dundas

et al., 2018). Furthermore, it was found that [NiFe]-hydrogenase had greater activity than [FeFe]-hydrogenase; therefore, [NiFe]-hydrogenase is more involved in the synthesis of bio-Pd NPs (Yang et al., 2020). Yang et al. (2020), stated that bio-Pd NPs on the outer membrane was produced by NADH-dehydrogenase, while production in the periplasm was provided by [FeFe]-hydrogenase and [NiFe]-hydrogenase (Yang et al., 2020). The hydrogenase mechanism of Bio-Pd NPs in the *Shewanella oneidensis* MR-1 bacteria cells was shown in detail at **Figure 2**.

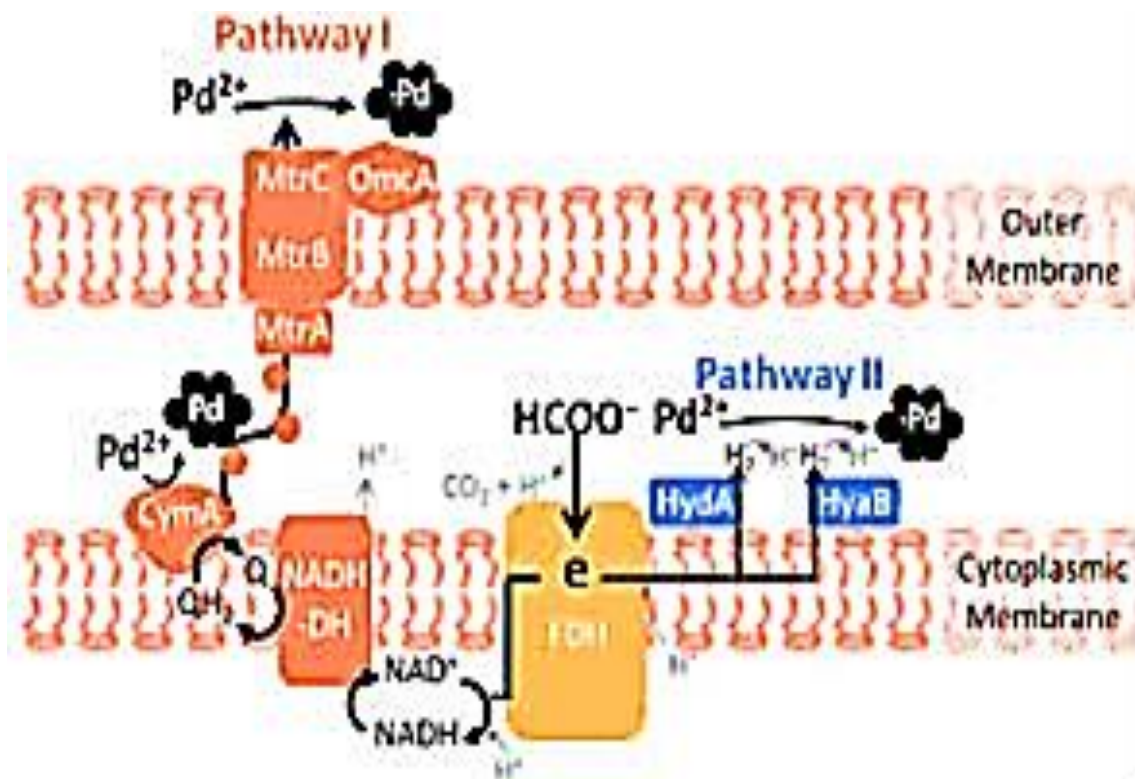


**Figure 2:** Hydrogenase mechanism of Bio-Pd NPs in the *Shewanella oneidensis* MR-1 bacteria cells

Deplanche et al. (2010) provided evidence that mainly [NiFe]-hydrogenase, localised in the periplasm, is essential for facilitating the production of bio-Pd NPs. This was supported by other researchers as well (Mikheenko et al., 2008; Deplanche et al., 2010; Shi et al., 2011; De Corte et al., 2012; Ng et al., 2013; Yang et al., 2020). This [NiFe]-hydrogenase enzyme can form and oxidate  $\text{H}_2(\text{g})$  in a bidirectional function. When oxidation of  $\text{H}_2(\text{g})$  occurs, electrons are released and used to reduce  $\text{Pd}^{2+}$  (Courtney et al., 2016; Yang et al., 2020). Anaerobic conditions are often required before reducing  $\text{Pd}^{2+}$  as only under these conditions [NiFe]-hydrogenase is expressed (Shi et al., 2011; Courtney et al., 2016). This enzyme can release electrons by oxidation of  $\text{H}_2(\text{g})$ ,  $\text{H}_2(\text{g})$  also needs to be added as an electron donor for the conversion (Ng et al., 2013a). The production of bio-Pd NPs does not only come from [NiFe]-hydrogenase, 50% of the converted  $\text{Pd}^{2+}$  comes from other enzymes (Ng et al., 2013a). This was due to the similarities between  $\text{Ni}^{+2}$  and  $\text{Pd}^{+2}$ , according to Deplanche et al. (2014). The  $\text{Ni}^{+2}$  is a key component for many metalloenzymes, that are located in the cytoplasm and will be simultaneously transported by the  $\text{Ni}^{+2}$  “trafficking system” through the cell membrane. Due to the chemical similarities  $\text{Pd}^{+2}$  is transported across the membrane in the same way (Deplanche et al., 2014). The  $\text{Pd}^{+2}$  taken

up by the cytoplasm is deposited as NPs, however, this cannot substitute for the  $\text{Ni}^{+2}$  function (Gomez-Bolivar et al., 2019a; Gomez-Bolivar et al., 2019b). Nevertheless, after the uptake and deposition of the bio-Pd NPs, the metabolic activity could be detected through flow cytometry (Omajali et al., 2019). Once the  $\text{Pd}^{+2}$  is taken up inside the cytoplasm the  $\text{Pd}^{+2}$  starts forming  $\text{Pd}^0$  “seeds”, the formation of these “seeds” results in a loss of cell viability (Gomez-Bolivar et al., 2019a; Gomez-Bolivar et al., 2019b). Besides the biological reduction of  $\text{Pd}^{+2}$ , the chemical conversion also appears in this production mechanism. The added electron donor can also be used for the chemical reduction of  $\text{Pd}^{+2}$  without the use of microorganisms. These chemical-produced NPs are going to attach to the existing bio-Pd NPs, causing particle aggregation (De Windt et al., 2006; Deplanche et al., 2014). Chemically produced NPs have a negative zeta potential and attract the  $\text{Pd}^{+2}$ , by the van der Waals forces, and finally attach to the newly formed bio-Pd NPs (Berg et al., 2009; Sathishkumar et al., 2009). The particle aggregation negatively influences the catalytic activity (De Windt et al., 2006). The bio-Pd NPs are often detected as NPs in spherical form, where the size can vary abundantly (Sahin and Gubbuk, 2022). Besides this, recently it was found that microbes were able to dissolve  $\text{Pd}^0$  which is an intermediate form of  $\text{Pd}^{+2}$  towards Pd NPs during

microbial reduction by *Shewanella oneidensis* MR-1 cells (Zheng et al., 2022). Furthermore, 2D structured nanomaterials of Pd were also discovered; nevertheless, the 2D structured Pd NPs are not synthesised with biological carriers, but are chemically produced (Xu et al., 2021). The presence of metals, like Pd, in microorganisms has a significant impact on the viability of the cells because of the high toxicity. Once the NPs are formed, the bacteria die (Suja et al., 2014). However, the toxicity of the metal to the microorganisms is strongly dependent on the type of metal, concentration, and microorganisms. In some cases, the presence of metals can enhance cellular viability which is strongly dependent on the concentration of the metal, by enhancing the decomposition of reactive oxygen species (ROS) (De Windt et al., 2006; Wu et al., 2011; Sakimoto et al., 2016; Ji et al., 2018; Chen and Chen, 2021). When high concentrations of metals are present, microorganisms tend to produce ROS due to the stress caused by the presence of the heavy metals (Yin and Gao, 2011; Chen and Chen, 2021; Joudeh et al., 2021). It was suggested that *Shewanella oneidensis* also produces ROS when heavy metals are present, causing damage to essential proteins responsible for transport and respiration inside the cell (Yin and Gao, 2011). The presence of ROS damage proteins which directly reduces the ability of the cells to survive or thrive. Second, it also damages proteins that can release irons in the cultures, resulting in a higher stimulation of ROS production and is more fatal because it occurs when the damaged cells are recovering (Yin and Gao, 2011). De Windt et al. (2006) observed that for 50 mg/l *Shewanella oneidensis* MR-1 the cells were inviable at a Pd<sup>+2</sup> concentration of 125 mg/l (De Windt et al., 2006; Chen and Chen, 2021). It was also found that bio-Pd NPs were more toxic for Gram-positive than Gram-negative bacteria (Adams et al., 2014). Nevertheless, depending on the type of metal and bacteria biological conversion can still occur independently of the viability of the bacterial cell due to the presence of

specific organic functional groups on the cell wall (Vijayaraghavan and Ashokkumar, 2017). This differential expression also occurred for the functional genes, whereof the highest changes can be found for genes responsible for amino acid transport and metabolism, carbohydrate transport and metabolism, transcription, post-translational modification, protein turnover, and chaperons. Compared to other heavy metals, Pd caused higher protein damage due to cross-linking, disruption of the 3D structures, and allosteric movements. It was found that the microorganism was still metabolic active, and hence viable after exposure to 100 µM sodium tetrachloropalladate, but not culturable. This is due to the downregulation of the repair genes and up-regulation of carbohydrate metabolism genes (Joudeh et al., 2021). However, it was found that higher resistance toward the toxicity of Pd can be solved by genetic modification. Nevertheless, genetic modification is expensive and labour-intensive.

### 3.2. Bio-Pd NPs Production Methods

Bio-Pd NPs production can be performed by using microorganisms, plants, and anaerobic sludge, respectively. Microorganisms are often used for production due to their lower cost and environmental sustainability (Mughal et al., 2021). The use of *Shewanella oneidensis* and *Desulfovibrio desulfuricans* are well known for their highly active production of nanocatalysts. However, after the production, an extra washing step is needed to remove the produced H<sub>2</sub>S which is poisonous to the catalyst (Lloyd et al., 1998; Wu et al., 2015; Courtney et al., 2016). In contrast, the toxification of the catalyst from H<sub>2</sub>S can be prevented by using *Escherichia coli* and *Rhodobacter sphaeroides* (Redwood et al., 2008; Deplanche et al., 2010). The production of bio-Pd NPs with *Shewanella oneidensis* MR-1 was explained in detail in **Figure 3**.

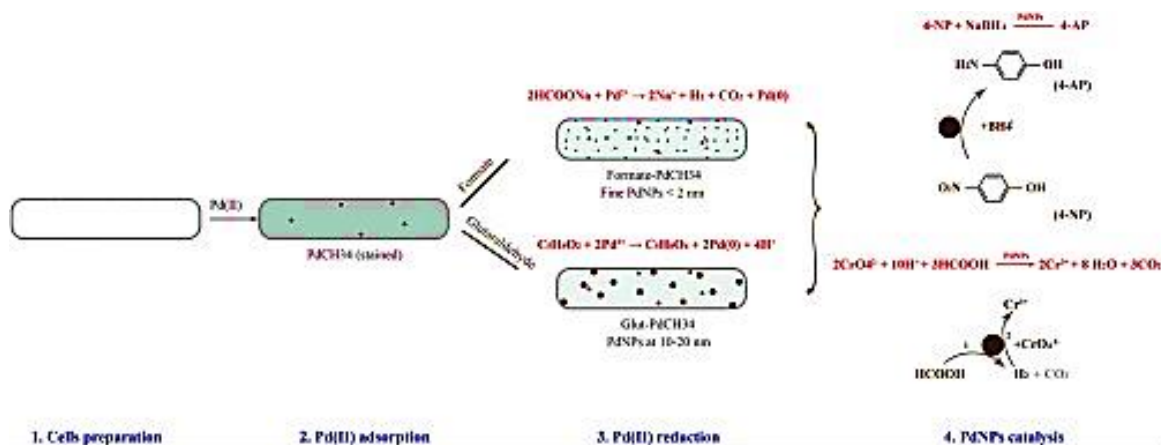


**Figure 3:** Production of bio-Pd NPs with *Shewanella oneidensis* MR-1

The formation of the bio-Pd NPs by Gram-negative or Gram-positive microorganisms is different due to cell wall differences which play an essential role by influencing the metals' binding onto the surface (Adams et al., 2014; Deplanche et al., 2014). Various Gram-negative and Gram-positive strains have been tested for the production of different-sized bio-Pd NPs, where a significant difference in size was found. The bio-Pd NPs produced by Gram-negative bacteria tend to outcome small NPs equally distributed around the cell wall. While in contrast, Gram-positive bacteria produce a few large NPs (Deplanche et al., 2014). This difference was not caused by the distinct metabolic activity, but potentially by biosorption. Sorption of Pd<sup>+2</sup> was higher for Gram-negative strains than for Gram-positive strains. Resulting in higher concentrations of Pd<sup>+2</sup> in the solution for Gram-positive bacteria. Subsequently, more chemical conversions are appearing, hence the generation of larger NPs (Deplanche et al., 2014). Plants are also often used for the production of bio-Pd NPs. Different plants and forms – (e.g., powder or extract) and complete parts of plants

(e.g., stem, leaf, root, fruit, flower, and seed) can be used (Sathishkumar et al., 2009; Siddiqi and Husen, 2016; Vijayaraghavan and Ashokkumar, 2017). They have the capability of accumulating metal ions that can be reduced to NPs (Bali et al., 2006; Vijayaraghavan and Ashokkumar, 2017). However, the use of entire plants is prevented, as this results in the production of NPs of different sizes and shapes throughout the plant. This is caused by the difference in penetration and localisation of the metal ions in the plant due to the diverse reduction capacities of the plant parts (Sharmila et al., 2017). Complex methods are needed to extract, purify, and increase the recovery of the particles (Bali et al., 2006; Sharmila et al., 2017; Vijayaraghavan and Ashokkumar, 2017). Therefore, plant extracts are often preferred in general due to the instant conversion of metals into NPs, absence of penetration, higher recovery, and less variation in size and shape (Makarov et al., 2014; Siddiqi and Husen, 2016; Shaik et al., 2017; Md Ishak et al., 2019). This is due to the functioning of biomolecules from the extracts as reducing and stabilising

agents (Shaik et al., 2017; Vijayaraghavan and Ashokkumar, 2017; Sarmah et al., 2019).

A new approach for bio-Pd NPs production can be obtained through anaerobic granular sludge which is mainly used to treat wastewater (Pat-Espadas et al., 2016; Quan et al., 2020). The benefit of using anaerobic granular sludge is (1) treatment of wastewater, (2) recovery of Pd<sup>+2</sup> from wastewater, and (3) the catalytic activity of the NPs. This is without any additional cost and energy (Quan et al., 2015a; Quan et al., 2015b; Quan et al., 2019). However, the reduction of Pd<sup>+2</sup> through anaerobic sludge is strongly dependent on the type of electron donor. Hence, different types of electron donors were tested. Nonetheless, only H<sub>2</sub>(g) and formate showed a biological and chemical reduction of Pd<sup>+2</sup> which was not found for pyruvate, lactate, acetate, and ethanol (Pat-Espadas et al., 2016). A part of the Pd<sup>+2</sup> present in the wastewater remained unconverted both biologically and chemically. Besides, the latter two mechanisms, the third mechanism of conversion occurred through biosorption of the metal ion which is the bonding between the Pd<sup>+2</sup> and sludge, by chemisorption (Pat-Espadas et al., 2016). Extracellular ligands induced this binding with weak acid organic functional groups associated with organomonometallic complexation (Gould and Genetelli, 1978; Alibhai et al., 1985; Pat-Espadas et al., 2016). This biosorption was also caused by the interaction between the organic functional groups on the cell wall (e.g., amine, amide, phosphoryl, and carboxyl groups) and the Pd<sup>+2</sup> (Fahmy et al., 2006; Rotaru et al., 2012; Pat-Espadas et al., 2016). However, an inhibitory effect was also observed on the microbial community due to the exposure of bacteria to Pd. The bio-Pd NPs affected the bacterial and archaeal community as well as the produced total volatile fatty acids (Pat-Espadas et al., 2016; Quan et al., 2020). When an increase in volatile fatty acids is present, this indicates a failure of the anaerobic sludge, more specifically the inhibition of the microbial community present in the sludge (Appels et al., 2008; Franke-Whittle et al., 2014). Volatile fatty acids are normally produced and used by the microorganisms present in the anaerobic sludge (Ahring et al., 1993; Appels et al., 2008). However, when there is an increase in the volatile acids, this indicates that some of the microorganisms are inhibited, consequently resulting in a decrease in pH and an inhibition of the other microorganisms that are present (Zaher et al., 2004). Hence, this inhibitory effect on the anaerobic sludge is undesired, as the sludge is responsible for treating the wastewater. This toxic effect is different for each microbial community in the granular sludge due to their characteristics and spatial organisation in the sludge. The bacterial community is present in the outer layer, while the methanogens are in the granular sludge's core (Hulshoff Pol et al., 2004). However, contradictory results were obtained regarding the inhibition effect on the different methanogenic archaeal communities—acetoclastic and hydrogenotrophic methanogens.

The disruption of the biological conversion of Pd<sup>+2</sup> can also be affected by the binding of Pd onto proteins or by the replacement of essential metals for the function of the proteins. This replaced or bound Pd can disrupt the enzyme function and structure which results in the loss of their essential functional proteins (Vallee BL, Ulmer, 1972; Quan et al., 2020).

### 3.3. The Catalytic Activity of Bio-Pd NPs

Reductions are needed to trigger the well-known catalytic activity of bio-Pd NPs such as dehalogenation or hydrogenation reactions. Therefore, different compounds can be used, such as pyruvate, lactate, acetate, formate, and H<sub>2</sub>(g) (Pat-Espadas et al., 2016; Cheng et al., 2017). Based on research, H<sub>2</sub>(g) is the most efficient electron donor to activate the dehalogenation or hydrogenation processes by the catalytic activity of the bio-Pd NPs. The Pd adsorbs H<sub>2</sub>(g) and converts it into atomic hydrogen which is very reactive as a reduction agent (Van Nevel et al., 2011; De Gusseme et al., 2012). The hydrogen radicals adsorbed onto the NPs contribute significantly to the high catalytic activity of bio-Pd NPs (De Windt et al., 2006; Hennebel et al., 2011). However, the catalytic efficiency of bio-Pd NPs can be influenced by (1) the size and distribution

of the NPs on the cell wall, and (2) the activation method of the bio-Pd NPs (Hou et al., 2017; Xiong et al., 2018).

Small bio-Pd NPs can be obtained without using extreme conditions and toxic chemicals through the presence of the biological carrier (De Windt et al., 2006). The size of the NPs has a direct influence on the catalytic activity (Zhou et al., 2006). Therefore, small NPs give a high ratio of surface area/volume which results in high surface energy combined with high reactivity (Hennebel et al., 2009a; Hennebel et al., 2009b; Leso and Iavicoli, 2018). This catalytic activity can be optimised by changing the size and distribution of the NPs. The aforementioned optimisation depends on the Pd/cell dry weight (CDW) ratio which affects the viability of the biological carrier, hence the microorganism (De Windt et al., 2006; Zhou et al., 2006; Gomez-Bolivar et al., 2019a; Gomez-Bolivar et al., 2019b). According to De Windt et al. (2006), and Hou et al. (2017), a lower Pd/CDW ratio gives a higher biological conversion of Pd<sup>+2</sup> into NPs. This results in small and uniformly distributed NPs throughout all the cells. On the contrary, a high ratio gives large NPs due to the abrupt death of cells because of the high Pd<sup>+2</sup> concentration, which is toxic, compared to the CDW (De Windt et al., 2006). Hence, a low ratio is desired when bio-Pd NPs are produced (De Windt et al., 2006; Hou et al., 2017).

Dehalogenation and hydrogenation by the catalytic activity of bio-Pd NPs occurs mainly through the addition of H<sub>2</sub>(g) as an electron donor. This can be optimised by changing the activation method (De Windt et al., 2006; Hennebel et al., 2009a; Hennebel et al., 2009b; Hennebel et al., 2010). Activation agents such as potassium hydroxide (KOH) and sodium hydroxide (NaOH) are often used as bioinorganic catalysts, due to their reaction ability with inert carbon materials that create desired pores in the carbon precursor (Świątkowski, 1999; Linares-Solano et al., 2012). Optimised catalytic activity of bio-Pd NPs is established by applying KOH as an activation agent. This method is altering the shape of microorganisms and Pd NPs, as the composition of the Pd NPs, by the thermal treatment of KOH. This thermal treatment carbonises the cells and starts the production of porous structures by guiding the reaction between KOH and the carbon (Świątkowski, 1999; Xiong et al., 2018). Two reaction mechanisms contribute to the formation of the large porous structure: (1) decomposition of functional groups of microorganisms resulting in a high porosity and surface area combined with the release of some volatiles [e.g. H<sub>2</sub>O(liq), CO<sub>2</sub>(g) and CO(g)]. Furthermore, (2) the release of H<sub>2</sub>O(liq) and CO<sub>2</sub>(g) is contributing as well, through the physical activation of CO<sub>2</sub>(g) and steam. The dispersed Pd NPs are spread throughout the carbon hybrid material. This stabilises the Pd NPs and facilitates the diffusion of the target compounds and electron donors to the catalyst's active sites. The elevated temperature also influences the Pd NPs by increasing the crystallinity of the NPs which showed a substantial effect on the catalytic performance. The advantages of this method are (1) an increase in dispersion of small NPs on the carrier, (2) having more binding sites and surface anchoring groups, and (3) enhancing the catalytic activity by improving the hydrophilicity of the nanostructures (Xiong et al., 2018). It is also possible to use hydrothermal processes to increase the activity, when producing alloys, such as PdAu alloys which contributes to the heteroatom doping of Pd and Au. To maintain and prevent aggregation from occurring, graphene oxide was used. The benefits of this process are (1) an increase in catalytic activity and (2) higher durability compared to commercial Pd/C NPs (Liu et al., 2016).

### 3.4. The Effect of Bio-Pd NPs on Electrochemical Systems

Fuel cell technologies present low carbon energy, high energy-density, zero-emission of CO<sub>2</sub>(g), and relatively easy production (Aki et al., 2005; Orozco et al., 2010; Quan et al., 2015a; Quan et al., 2015b). Two types of cell technologies are commonly used, hence electrochemical cells: (1) MFC and (2) Microbial Electrolysis Cell (MEC). Lately, research has been focusing on the use of these cells combined with catalysts due to their higher efficiency. One of the commonly used elements for this is Pd (Saravanakumar et al., 2016; Wang et al., 2019; Tahernia et al., 2020). It

has been proven that the use of Pd can enhance the reaction rate, conductivity, and charge transfer, hence the generation of current (Cheng et al., 2017; Wang et al., 2019). The bio-Pd NPs have also been applied in electrochemical cells (Cheng et al., 2017).

The MFC is a bio-electrochemical system that uses microorganisms to transform chemical energy into electricity (Lovley, 2008; Chaturvedi et al., 2016). Only electroactive bacteria can be used through the process, as they serve as biocatalysts, hence generating bio-energy (Kumar et al., 2016; Thapa et al., 2022). These microorganisms transfer electrons, directly (DET) or mediated (MET), to the electrode, by oxidising organic compounds, e.g., glucose, formate, and acetate, which serve as carbon sources (Kumar et al., 2016). By oxidising the organic compounds, microorganisms make electrons available. This is transferred to the anode, and from there to the cathode through a circuit where they reduce the oxidant (Allen et al., 1993; Tahernia et al., 2020). Hence, the efficiency of this transfer from chemical to electricity dramatically depends on the anode. The anode is the primary location where the microorganisms attach (Watanabe et al., 2008; Quan et al., 2015a; Quan et al., 2005b).

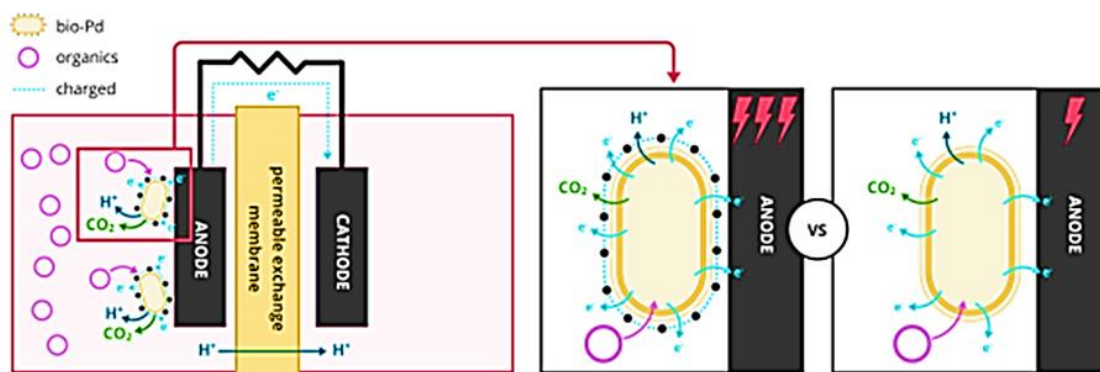


**Figure 4:** Coating anode with bio-Pd in the microbial electrochemical fuel cell (MFC) system to increase the generation of energy. The figure was adapted from Hou et al. (2017).

Besides, the loading of bio-Pd NPs on the electrode is the type of organic compound also essential for improving the generation of bio-energy. Quan et al. (2015a), and Matsena et al. (2020) reported the inadequate use of glucose to improve bio-energy generation. This is due to the absence of direct electro-oxidation by bio-Pd NPs and hindered utilisation from the microorganisms to generate power (Wu et al., 2011; Quan et al., 2015a; Wu et al., 2018; Matsena et al., 2020; Tahernia et al., 2020). Hence, it is important to use a suitable organic compound for the electro- and microbial oxidation. The advantage of having bio-Pd NPs in the electrochemical systems are (1) the presence of microorganisms to oxidise the organic compounds and (2) bio-Pd NPs to catalyse the oxidation of the organic compounds further which improves the energy generation (Yong et al., 2002; Quan et al., 2015a; Quan et al., 2005b; Matsena et al., 2020).

While energy is produced in MFC, MEC partially reverses the process using the energy for the production of  $H_2(g)$  or degradation of contaminants. The  $H_2(g)$  is considered an alternative to fossil fuels (Shafiee and Topal, 2009). The advantage of this system is that there is no emission of  $CO_2(g)$ , clean end-products, and has high-energy-density (Orozco et al., 2010; Abdalla et al., 2018). The MEC principles are based on the hydrogen evolution reaction (HER) which is a cathodic reaction that electrochemically split water in the cathode (Seh et al., 2017). The HER process is a combination of hydrogen adsorption and desorption from the electrode surface where an optimal level of bonding strength between catalytic surface and hydrogen atoms needs to be achieved aiming not to favour one step over the other. If the bonding between hydrogen and the catalytic surface is weak, adsorption is inadequate, and the overall efficiency would suffer. Besides, if the bonding between hydrogen and the electrocatalytic surface is too strong it is not desorbed

Therefore, a variety of carbon-based materials enhance bacterial attachment and hence the transfer of electrons (Quan et al., 2015a; Quan et al., 2005b). Recently, attention is gained to the use of bio-Pd NPs to cover the anode. This increases the performance of the MFC, by enhancing the generation of current. The combination of bio-Pd NPs with the anode establishes the use of the MFC for electro-oxidation, here, Pd present in the anode is electrocatalytic active (Saravanakumar et al., 2016). The bio-Pd NPs serve as an electroactive catalyst that enables the degradation of organic compounds which increases the number of electrons (Quan et al., 2015a; Quan et al., 2005b).

This improves the transfer of electrons and reduction in resistance of charge transfer in the electrochemical systems (Figure 4). It was found that a higher loading of bio-Pd NPs could increase the Coulombic efficiency from 14% (1 mg bio-Pd/cm<sup>2</sup>) to 31% (2 mg bio-Pd/cm<sup>2</sup>) compared to the anode without bio-Pd NPs (Quan et al., 2015a). Matsena et al. (2020), also found an increase in bio-energy generation from 31.1% to 59.6%, with 2 to 4 mg bio-Pd/cm<sup>2</sup>, respectively. This was compared to the electrode without bio-Pd NPs (Matsena et al., 2020).

from the surface effectively, lowering overall efficiency (Safizadeh et al., 2015). To increase this reaction, a catalyst can be used, e.g. platinum and Pd, by coating the metal onto an electrode (Yuan and He, 2017). The Pd is often used because of having the best properties in hydrogen-storage, under suitable conditions Pd adsorbs more than 900 times its volume of hydrogen (Dekura et al., 2019; Wang et al., 2019; Hou et al., 2020). It also plays an important role in the redox reaction. The use of bio-Pd accelerates the reaction as it serves as a catalyst which increases the HER and, consequently, removes contaminants. This is due to the higher concentration of electron donors which can be used for catalytic activity (Hou et al., 2016; Hou et al., 2017). However, the characteristics of the bio-Pd NPs to achieve a high catalytic activity are different for electrochemical systems and in suspension (De Windt et al., 2006; Hou et al., 2017). In electrochemical systems, increased conductivity is obtained by interconnecting all bio-Pd NPs, and hence, smaller NPs in size are not crucial. This results in the activation of every particle in the electrochemical system and thus an enhanced catalytic activity. Therefore, the electrochemical active surface area (ECSA) is an important parameter in conductivity and is directly influencing the catalytic performance (Hou et al., 2017). However, the size does play an important role in the catalytic activity of bio-Pd NPs in suspension (De Windt et al., 2006). The highest catalytic activity is obtained when small NPs are present. This is due to the ratio in size of NPs versus uncovered areas of the cell with Pd (Hou et al., 2017). Hou et al. (2017), observed the difference in catalytic activity between bio-Pd in electrochemical systems and suspensions. The bio-Pd NPs with Pd/CDW ratio=6/1 showed the biggest NPs of  $54.3 \pm 16.4$  nm, while  $25.8 \pm 7.8$  nm particles were obtained for the 3/1 ratio. As indicated by De Windt et al. (2006), the ratio of Pd/CDW determines the size, extracellular distribution, and coverage of

the Pd NPs in the cell. Nevertheless, the highest current densities were obtained due to the high ECSA, and hence, favourable catalytic activity in the electrochemical system was reached with the NPs produced with Pd/CDW ratio=6/1 (De Windt et al., 2006; Hou et al., 2017). However, the highest catalytic activity of bio-Pd in suspension was obtained for Pd/CDW ratio=3/1. Hence, high coverage of Pd NPs on cells can negatively impact the catalytic activity depending on the use (Hou et al., 2017).

### 3.5. Bio-Pd NPs Characteristics

#### 3.5.1. The Results of Transmission Electron Microscopy (TEM) Analysis

The TEM images of bio-Pd NPs at the *Shewanella oneidensis* MR-1 cell surface was observed in micromorphological structure level in bio-electrochemical cell assisted production of bio-Pd NPs with *Shewanella oneidensis* MR-1 bacteria for the catalytic removal of OFX and DOX micropollutants in pharmaceutical industry wastewaters (**Figure 5**).

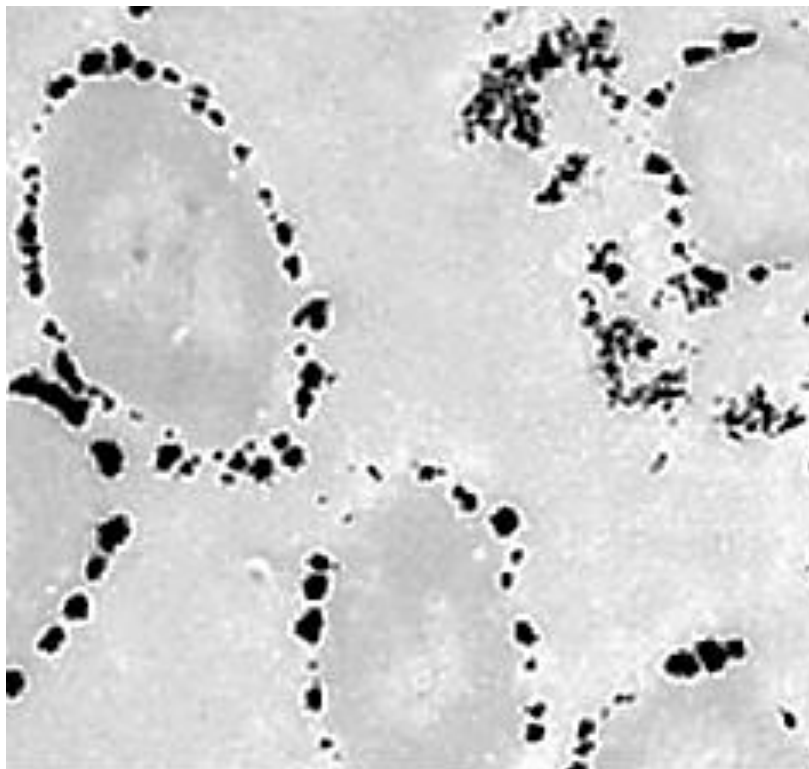


**Figure 5:** TEM images of bio-Pd NPs at the *Shewanella oneidensis* MR-1 cell surface in micromorphological structure level in bio-electrochemical cell assisted production of bio-Pd NPs with *Shewanella oneidensis* MR-1 bacteria for the catalytic removal of OFX and DOX micropollutants in pharmaceutical industry wastewaters.

#### 3.5.2. The Results of Field Emission Scanning Electron Microscopy (FESEM) Analysis

The morphological features of pure g-C<sub>3</sub>N<sub>4</sub> NPs, pure CeO<sub>2</sub> NPs and g-C<sub>3</sub>N<sub>4</sub>/CeO<sub>2</sub> NCs were characterized through FE-SEM images (**Figure 6**). The FESEM images of untreated pure *Shewanella oneidensis* MR-1 bacteria was shown in pharmaceutical industry wastewater (**Figure 6a**). The FESEM images of bio-Pd NPs loaded with *Shewanella oneidensis*

MR-1 cell surface were observed in bio-electrochemical cell assisted production of bio-Pd NPs with *Shewanella oneidensis* MR-1 bacteria for the catalytic removal of OFX micropollutants in pharmaceutical industry wastewaters (**Figure 6b**). The FESEM images of bio-Pd NPs loaded with *Shewanella oneidensis* MR-1 cell surface were observed in bio-electrochemical cell assisted production of bio-Pd NPs with *Shewanella oneidensis* MR-1 bacteria for the catalytic removal of DOX micropollutants in pharmaceutical industry wastewaters (**Figure 6c**).

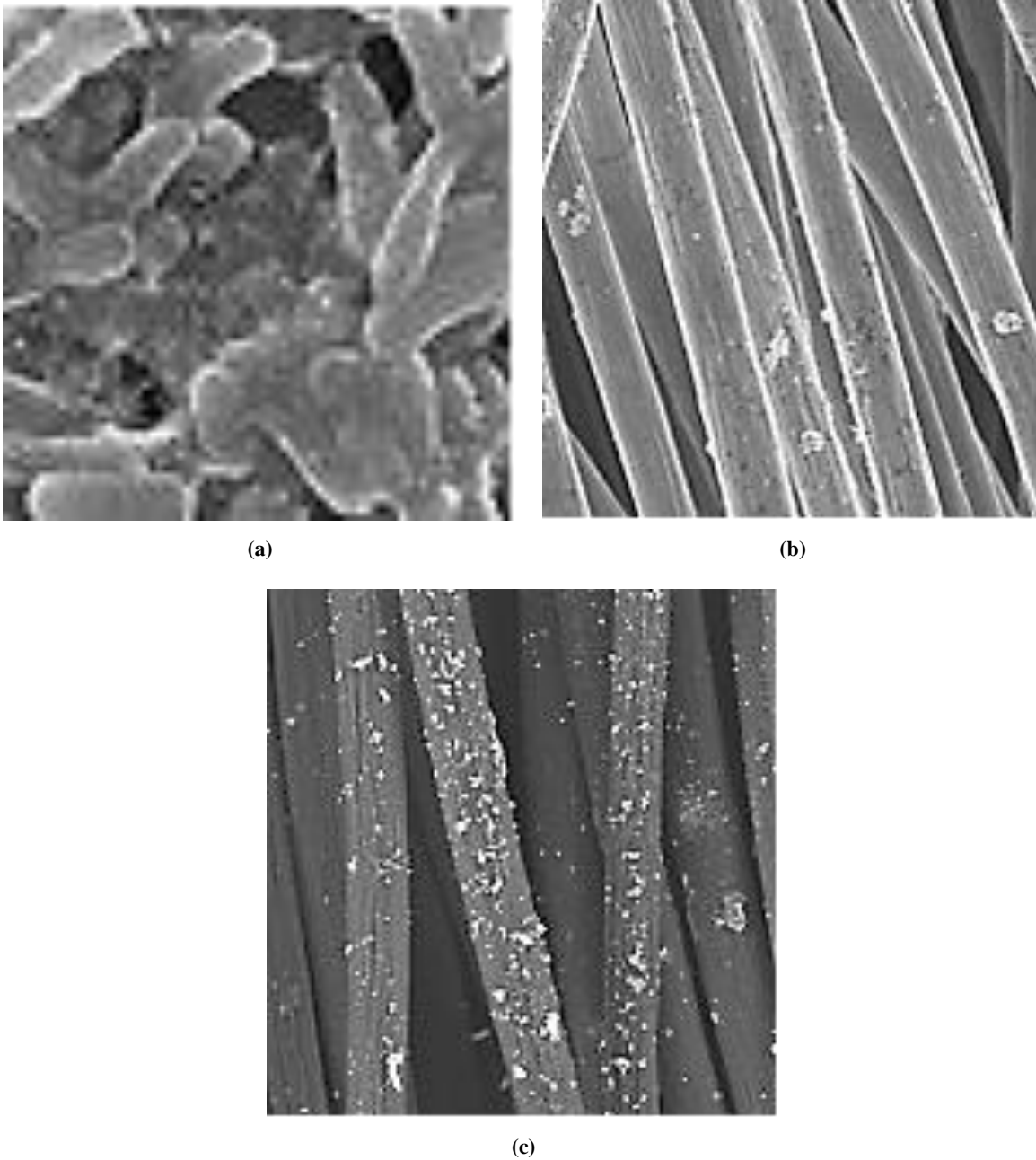


**Figure 6:** FESEM images of (a) untreated pure *Shewanella oneidensis* MR-1 bacteria, (b) after bio-electrochemical cell assisted production of bio-Pd NPs with *Shewanella oneidensis* MR-1 bacteria for the catalytic removal of OFX micropollutants and (c) after bio-electrochemical cell assisted production of bio-Pd NPs with *Shewanella oneidensis* MR-1 bacteria for the catalytic removal of DOX micropollutants in pharmaceutical industry wastewaters

### 3.5.3. The Results of Energy Dispersive X-Ray (EDX) Spectroscopy Analysis

The EDX analysis of bio-Pd NPs was also performed to investigate in the bio-electrochemical cell assisted production of bio-Pd NPs with

*Shewanella oneidensis* MR-1 bacteria for the catalytic removal of OFX and DOX micropollutants in pharmaceutical industry wastewaters (Figure 7).

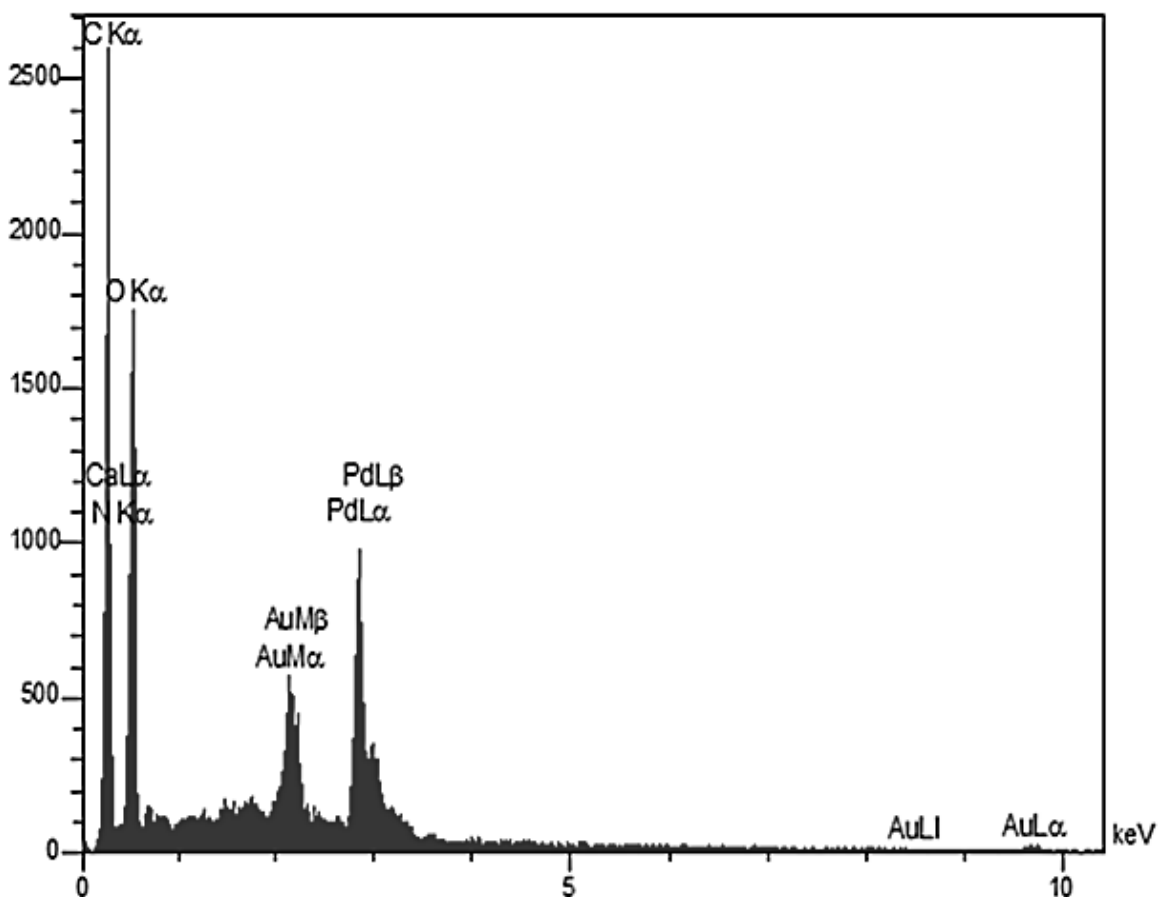
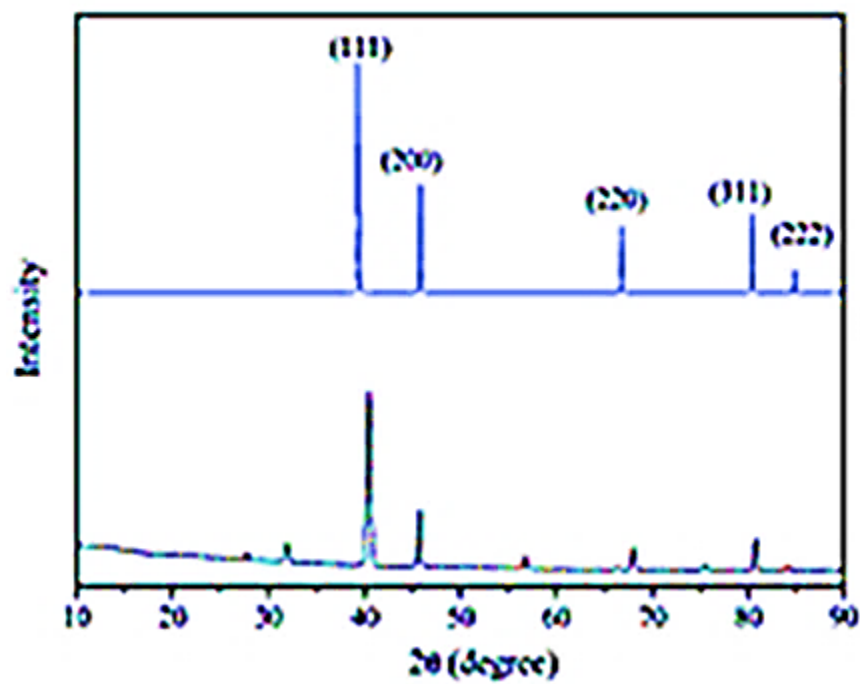


**Figure 7:** EDX spectrum of bio-Pd NPs in the bio-electrochemical cell assisted production of bio-Pd NPs with *Shewanella oneidensis* MR-1 bacteria for the catalytic removal of OFX and DOX micropollutants in pharmaceutical industry wastewaters

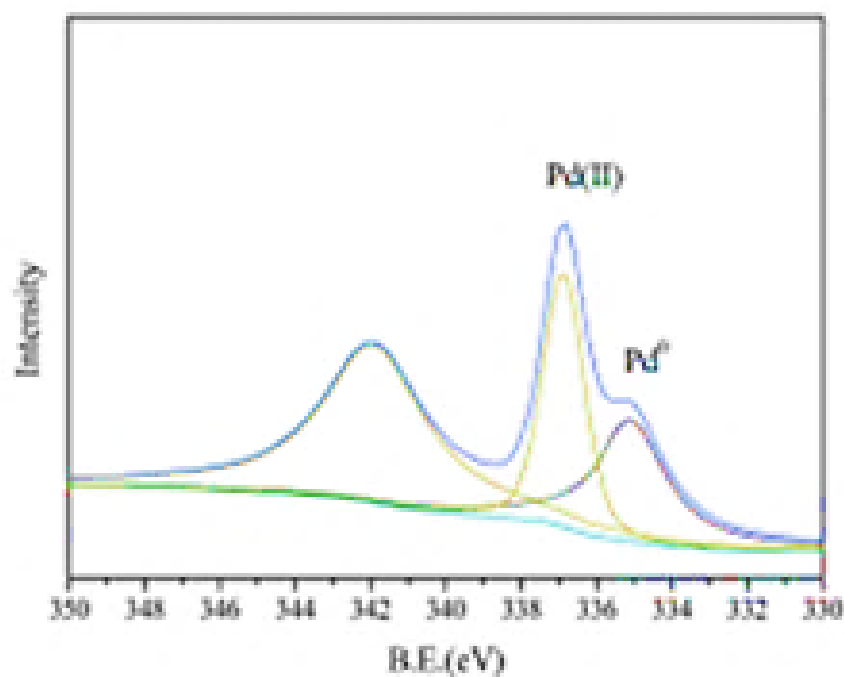
### 3.5.4. The Results of X-Ray Diffraction (XRD) Analysis and X-Ray Photoelectron Spectroscopy (XPS) Analysis

The results of XRD analysis was observed to bio-Pd NPs, in the bio-electrochemical cell assisted production of bio-Pd NPs with *Shewanella oneidensis* MR-1 bacteria for the catalytic removal of OFX and DOX micropollutants in pharmaceutical industry wastewaters (**Figure 8a**). The characterization peaks were found at  $2\theta$  values of  $39.25^\circ$ ,  $46.10^\circ$ ,  $68.17^\circ$ ,

$80.07^\circ$  and  $84.46^\circ$ , respectively, and which can also be indexed as (111), (200), (220), (311) and (222), respectively, implying g-C<sub>3</sub>N<sub>4</sub>/CeO<sub>2</sub> NCs in pharmaceutical industry wastewater with photocatalytic degradation process for OFX antibiotic removal (**Figure 8a**). The XPS analysis of bio-Pd NPs was also performed to investigate in the bio-electrochemical cell assisted production of bio-Pd NPs with *Shewanella oneidensis* MR-1 bacteria for the catalytic removal of OFX and DOX micropollutants in pharmaceutical industry wastewaters (**Figure 8b**).



(a)



(b)

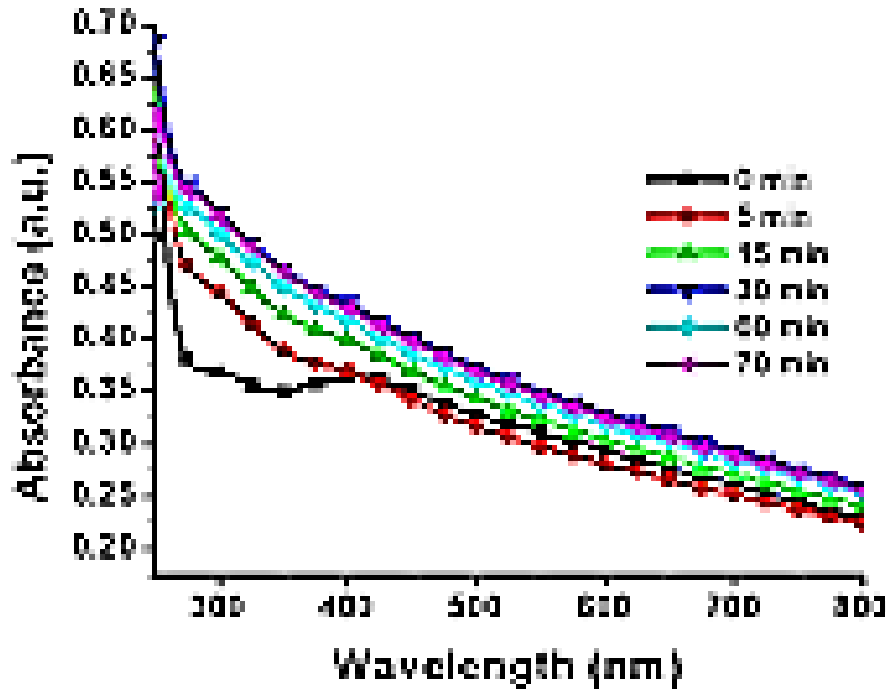
**Figure 8:** (a) XRD spectra of bio-Pd NPs and (b) XPS spectra of bio-Pd NPs in the bio-electrochemical cell assisted production of bio-Pd NPs with *Shewanella oneidensis* MR-1 bacteria for the catalytic removal of OFX and DOX micropollutants in pharmaceutical industry wastewaters

### 3.5.5. Inductively Coupled Plasma Mass Spectrometry (ICP-MS) Analysis

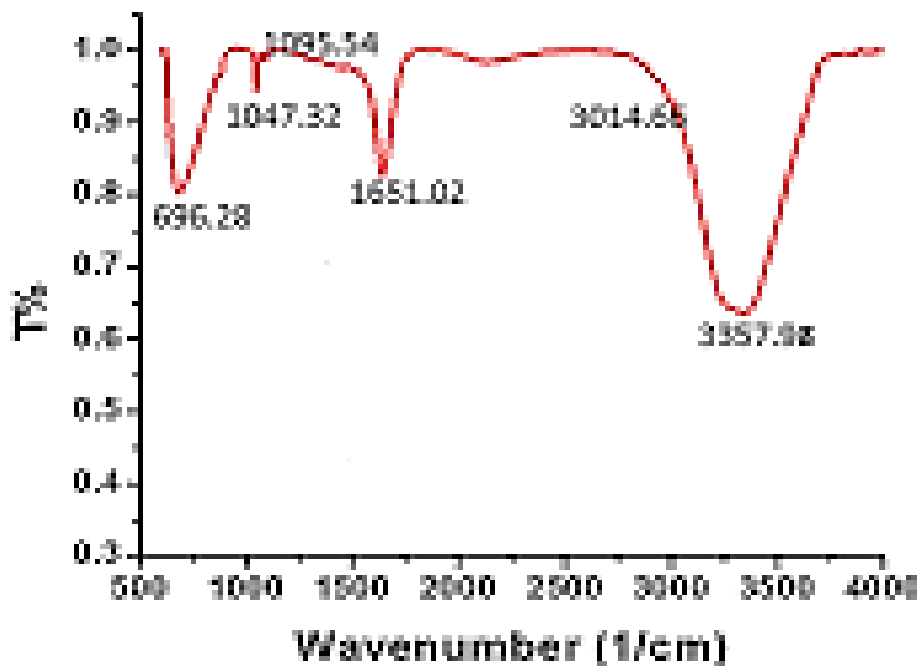
The ICP-MS analysis of bio-Pd NPs was also performed to investigate in the bio-electrochemical cell assisted production of bio-Pd NPs with *Shewanella oneidensis* MR-1 bacteria for the catalytic removal of OFX and DOX micropollutants in pharmaceutical industry wastewaters (Figure

9). After 70 min bio-in the bio-electrochemical cell assisted production of bio-Pd NPs with *Shewanella oneidensis* MR-1 bacteria was shown in Figure 9a. The main peaks of ICP-MS spectrum for bio-Pd NPs NPs was observed at 696.28 1/cm, 1047.32 1/cm, 1095.34 1/cm, 1651.02 1/cm, 3014.66 1/cm and 3357.95 1/cm wavenumber, respectively

(Figure



(a)



(b)

**Figure 9:** ICP-MS spectra of (a) after 70 min bio-in the bio-electrochemical cell assisted production of bio-Pd NPs with *Shewanella oneidensis* MR-1 bacteria, and (b) for the catalytic removal of OFX and DOX micropollutants in pharmaceutical industry wastewaters

**3.5.6. The Results of Fourier Transform Infrared Spectroscopy (FTIR) Analysis**

The FTIR spectrum of OFX and DOX micropollutants was obtained after catalytic removals with Bio-Pd NPs in *Shewanella oneidensis* MR-1, respectively, in pharmaceutical industry wastewater (Figure 10). The main peaks of FTIR spectrum for OFX catalytic removal with Bio-Pd NPs

in *Shewanella oneidensis* MR-1 (red spectrum) was observed at 3800 1/cm, 3150 1/cm, 2880 1/cm, 2250 1/cm, 1800 1/cm, 1500 1/cm, 1400 1/cm, 1320 1/cm, 1170 1/cm, 1000 1/cm, 980 1/cm, 970 1/cm, 820 1/cm, 750 1/cm and 500 1/cm wavenumber, respectively (**Figure 10a**). The main peaks of FTIR spectrum for DOX catalytic removal with Bio-

Pd NPs in *Shewanella oneidensis* MR-1 (blue spectrum) was obtained at 3750 1/cm, 3100 1/cm, 2800 1/cm, 2740 1/cm, 2400 1/cm, 1750 1/cm, 1580 1/cm, 1500 1/cm, 1360 1/cm, 1290 1/cm, 1000 1/cm and 750 1/cm wavenumber, respectively (**Figure 10b**).

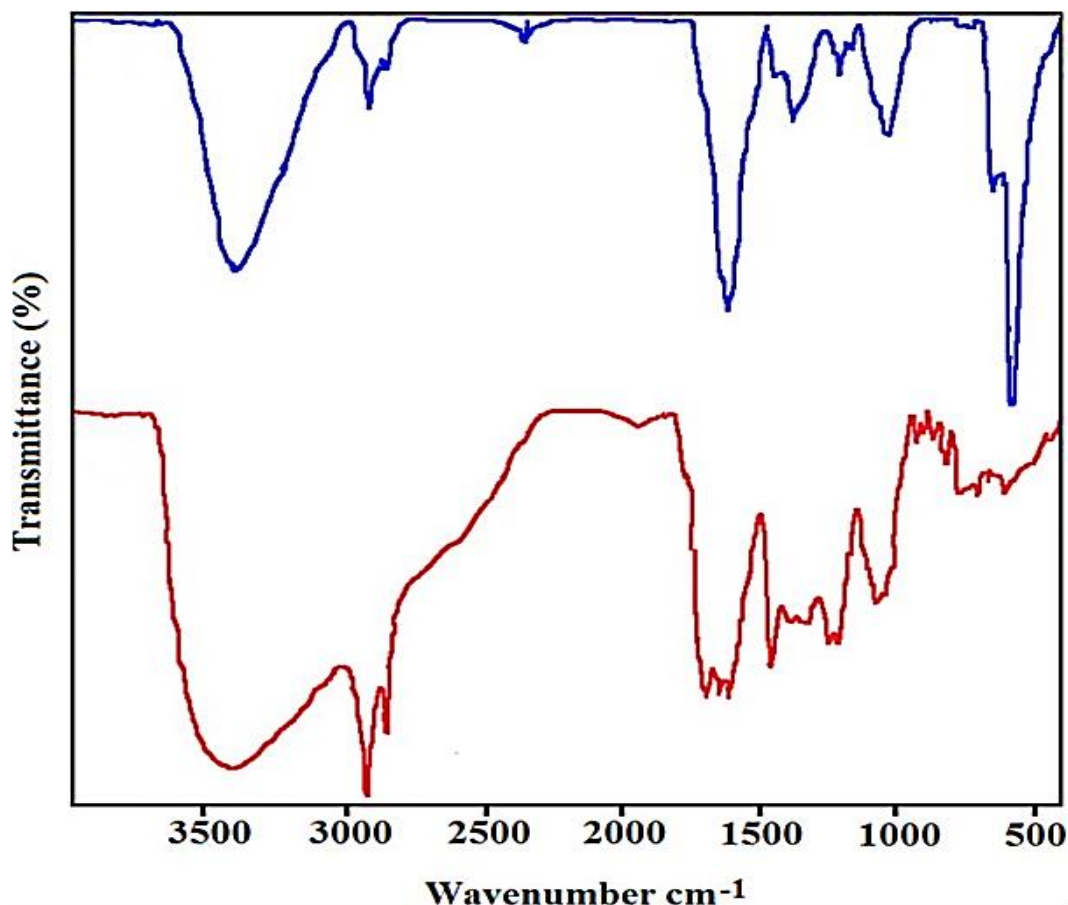


**Figure 10:** FTIR spectrum of (a) OFX catalytic removal with Bio-Pd NPs in *Shewanella oneidensis* MR-1 (red spectrum), (b) DOX catalytic removal with Bio-Pd NPs in *Shewanella oneidensis* MR-1 (blue spectrum), respectively, in pharmaceutical industry wastewater.

### 3.5.6. The Results of Diffuse reflectance UV-Vis Spectra (DRS) Analysis

The DRS spectrum of pure Bio-Pd NPs and bio-Pd NPs with Bio-Pd NPs in *Shewanella oneidensis* MR-1 cells was observed after catalytic removals of OFX and DOX micropollutants in pharmaceutical industry wastewater (**Figure 11**). First, the DRS spectra of pure Bio-Pd NPs were

obtained in the wavelength range from 250 nm to 500 nm using diffuse reflectance UV-Vis spectra (**Figure 11a**). Absorption peaks were observed at wavelengths of 310 nm for pure bio-Pd NPs (red pattern) (**Figure 11a**), 300 nm for bio-Pd NPs in *Shewanella oneidensis* MR-1 cells (blue pattern) (**Figure 11b**), respectively, after catalytic removals of OFX and DOX micropollutants in pharmaceutical industry wastewater

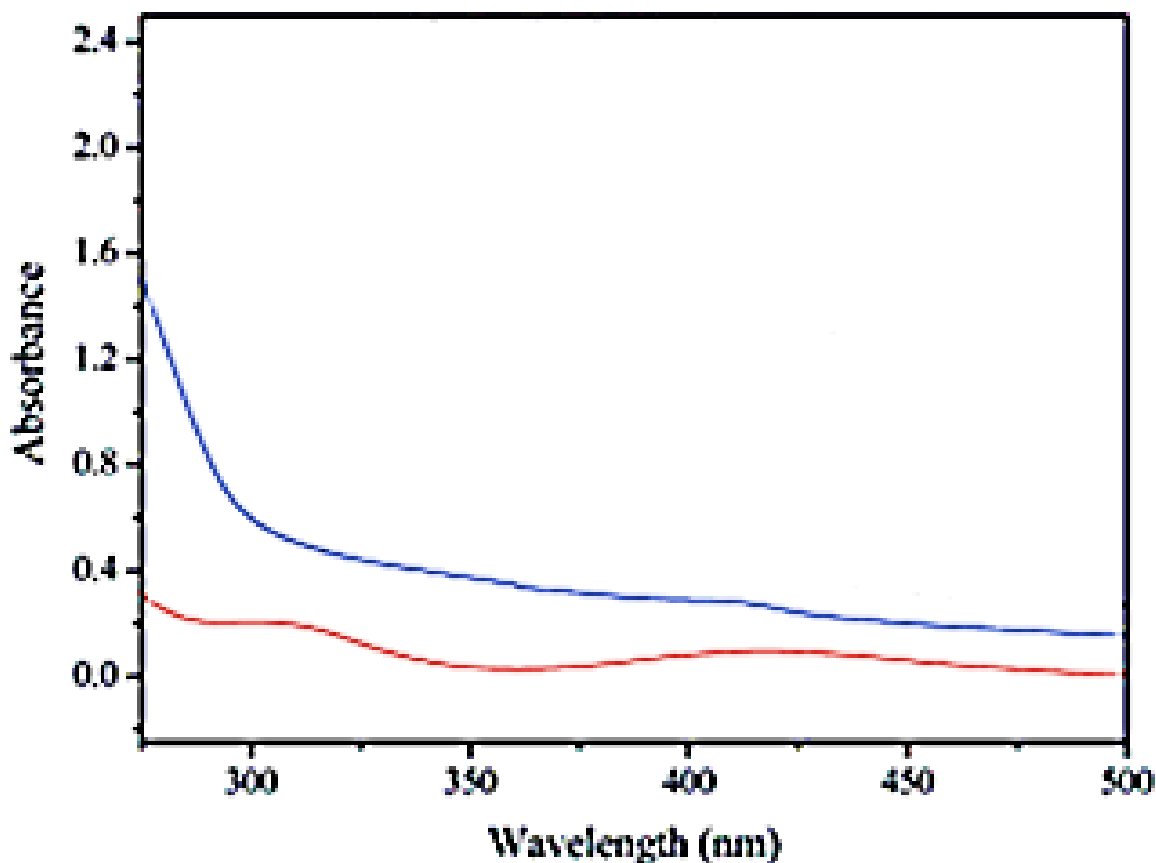


**Figure 11:** The DRS spectrum of (a) pure Bio-Pd NPs (red pattern) (b) bio-Pd NPs with Bio-Pd NPs in *Shewanella oneidensis* MR-1 cells (blue pattern), respectively, catalytic removals of OFX and DOX micropollutants in pharmaceutical industry wastewater.

### 3.6. The Reaction Kinetics of OFX Antibiotic

The reaction kinetics OFX were investigated using the Langmuir–Hinshelwood first-order kinetic model, expressed by Eddy et al. (2015), as following **Equation (1)**:

$$r_o = \frac{-dC}{dt} = kC \quad (1)$$

where;  $r_o$ : denotes the initial catalytic degradation reaction rate (mg/l.min), and  $k$ : denotes the rate constant of a first-order reaction. At the beginning of the reaction,  $t = 0$ ,  $C_t = C_0$ , the equation can be obtained after integration as following **Equation (2)**:

$$\ln \frac{C}{C_0} = -kt \quad (2)$$

where;  $C_0$  and  $C$ : are the initial and final concentration (mg/l) of OFX; the solution at  $t$  (min) and  $k$  (1/min) are the rate constant.

The correlation coefficients had  $R^2$  values greater than 0.9, as a result, the first-order kinetic model fit the experimental data well. The first-order rate constants ( $k$ ) were determined from the slope of the linear plots.

### 3.7. The Reaction Kinetics of DOX Antibiotic

DOX micropollutants removal using catalytic degradation can be described using a pseudo first-order reaction kinetic model (**Equation 3**) (Al-Hamadani et al., 2016; Villegas-Guzman et al., 2017; Monteagudo et al., 2018). However, a complete linear relationship was not observed for a first-order kinetic law and pollutants elimination could not be characterized by a single rate constant.

$$r = -\frac{dC}{dt} = k_0C \quad (3)$$

where;  $r$ : is the initial degradation rate ( $\mu\text{mol/l.min}$ ),  $k_0$ : is the pseudo-rate constant (1/min) and  $C$ : is the pollutant initial concentration ( $\mu\text{mol/l}$ ).

A Langmuir type mechanism model indicates that organic molecules adsorb and desorb from the liquid interface layer surrounding of the cavitation bubble, reaching a pseudo-steady state, and the degradation rate ( $r$ ) can be represented by **Equation 4** (Okitsu et al., 2005):

$$r = \frac{k_0KC}{1+KC} \quad (4)$$

where;  $r$ : is the initial degradation rate ( $\mu\text{mol/l.min}$ ),  $k_0$ : is the pseudo-rate constant ( $\mu\text{mol/l.min}$ ),  $C$ : is the pollutant initial concentration ( $\mu\text{mol/l}$ ) and  $K$ : is the equilibrium constant of the target compound at the interfacial region ( $l/\mu\text{mol}$ ). [

Thus, the degradation rate is the sum of the rates in the bulk and in the interface layer and can be expressed by the **Equation 5** (Serpone et al., 1994).

$$r = k_b + \frac{k_0KC}{1+KC} \quad (5)$$

where;  $k_b$ : is a constant representing the rate of decomposition in the bulk liquid ( $\mu\text{mol/l.min}$ ),  $r$ : is the initial degradation rate ( $\mu\text{mol/l.min}$ ),  $k_0$ : is the pseudo-rate constant ( $\mu\text{mol/l.min}$ ),  $C$ : is the pollutant initial concentration ( $\mu\text{mol/l}$ ) and  $K$ : is the equilibrium constant ( $l/\mu\text{mol}$ ) (Serpone et al., 1994).

Data indicates that the experimental results fit better ( $> 0.98$  higher coefficient of determination  $R^2$ ) with the model proposed by Serpone et

al. (1994) in comparison with the Okitsu et al. (2005) model and the pseudo first-order kinetics model.

### 3.7. Effect of Increasing pH values for OFX and DOX Catalytic Removals with Bio-electrochemical Cell Assisted Production of Bio-Pd NPs with *Shewanella oneidensis* MR-1 Bacteria in Pharmaceutical Industry Wastewater

Increasing pH values (pH=3.0, pH=4.0, pH=6.0, pH=7.0, pH=9.0 and pH=11.0, respectively) was examined during catalytic degradation process with bio-electrochemical cell assisted production of bio-Pd NPs

with *Shewanella oneidensis* MR-1 bacteria as a bio-electrochemical cell catalyts in pharmaceutical industry wastewater for OFX catalytic removal (Figure 12). 66%, 84%, 95%, 55% and 43% OFX removal efficiencies was measured at pH=3.0, pH=4.0, pH=7.0, pH=9.0 and pH=11.0, respectively, after 24 h catalytic degradation time, at 25°C (Figure 12). The maximum 99% OFX removal efficiency was obtained during photocatalytic degradation process in pharmaceutical industry wastewater, after 24 h catalytic degradation time, at pH=6.0 and at 25°C, respectively (Figure 12).

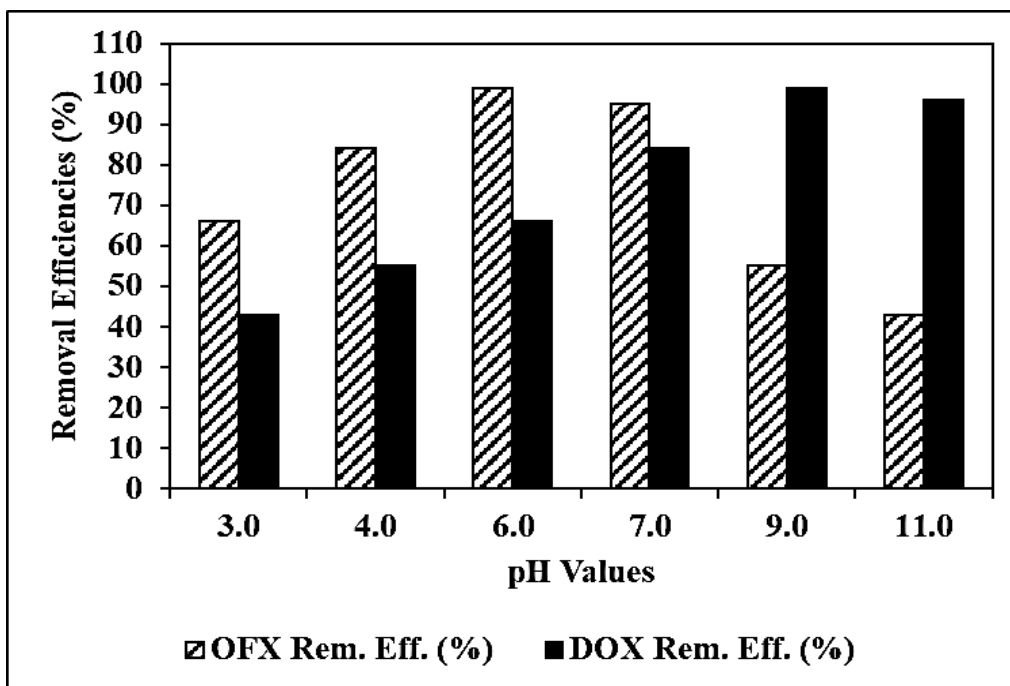


**Figure 12:** Effect of increasing pH values for OFX and DOX catalytic removals with bio-electrochemical cell assisted production of bio-Pd NPs with *Shewanella oneidensis* MR-1 bacteria as a bio-electrochemical cell catalyts in pharmaceutical industry wastewater after 24 h catalytic degradation time, at 25°C, respectively.

Increasing pH values (pH=3.0, pH=4.0, pH=6.0, pH=7.0, pH=9.0 and pH=11.0, respectively) was examined during catalytic degradation process with bio-electrochemical cell assisted production of bio-Pd NPs with *Shewanella oneidensis* MR-1 bacteria as a bio-electrochemical cell catalyts in pharmaceutical industry wastewater for DOX removal (Figure 12). 43%, 55%, 66%, 84% and 96% DOX removal efficiencies was measured at pH=3.0, pH=4.0, pH=6.0, pH=7.0 and pH=11.0, respectively, after 24 h catalytic degradation time, at 25°C (Figure 12). The maximum 99% DOX removal efficiency was obtained during photocatalytic degradation process in pharmaceutical industry wastewater, after 24 h catalytic degradation time, at pH=9.0 and at 25°C, respectively (Figure 12).

### 3.9. Effect of Increasing OFX and DOX Concentrations for OFX and DOX Catalytic Removals with Bio-electrochemical Cell

#### Assisted Production of Bio-Pd NPs with *Shewanella oneidensis* MR-1 Bacteria in Pharmaceutical Industry Wastewater

Increasing OFX concentrations (5 mg/l, 15 mg/l, 30 mg/l and 45 mg/l) were operated during catalytic degradation process with bio-electrochemical cell assisted production of bio-Pd NPs with *Shewanella oneidensis* MR-1 bacteria as a bio-electrochemical cell catalyts in pharmaceutical industry wastewater, at pH=6.0, after 24 h catalytic degradation time, at 25°C, respectively (Figure 13). 84%, 93% and 75% OFX removal efficiencies were obtained to 5 mg/l, 15 mg/l and 45 mg/l OFX concentrations, respectively, after 24 h catalytic degradation time, at pH=6.0 and at 25°C (Figure 13). The maximum 99% OFX removal efficiency was found with catalytic degradation process in pharmaceutical industry wastewater, at 30 mg/l OFX, after 24 h catalytic degradation time, at pH=6.0 and at 25°C, respectively (Figure 13).

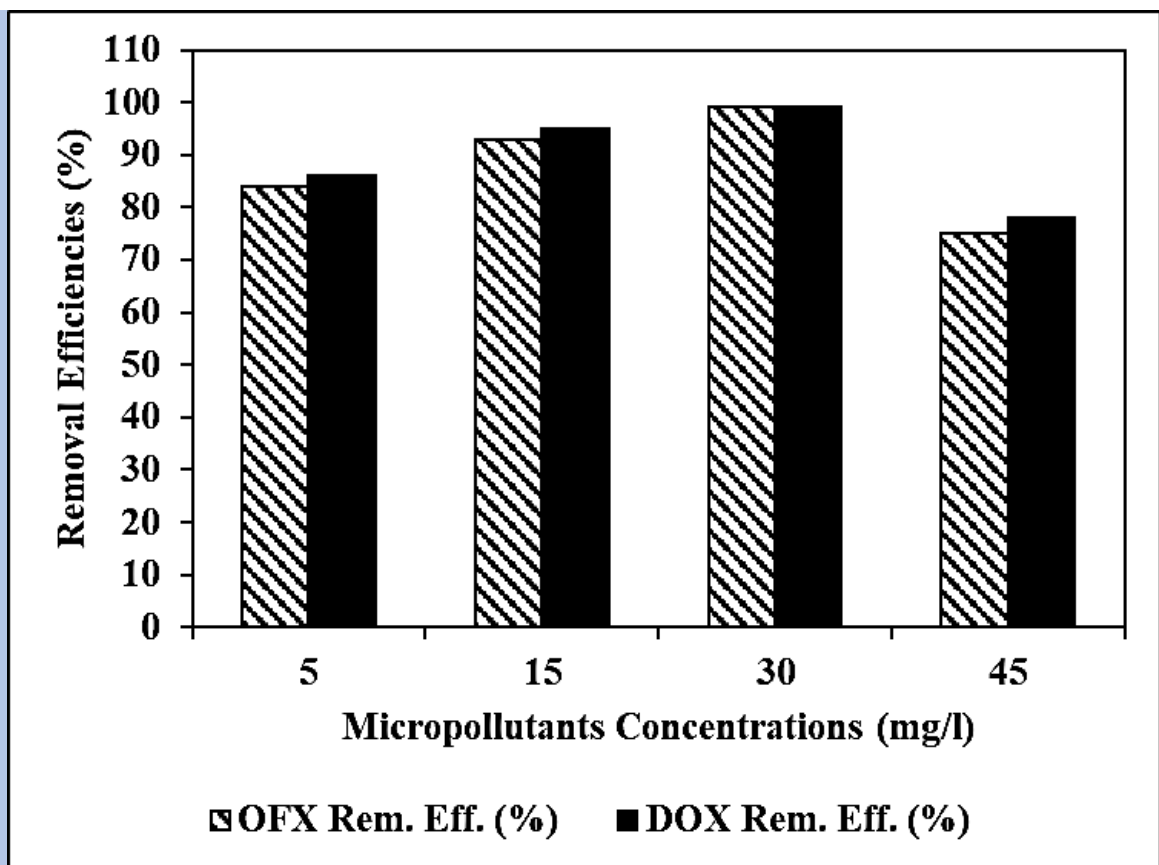


**Figure 13:** Effect of increasing OFX and DOX concentrations for OFX and DOX catalytic removals with bio-electrochemical cell assisted production of bio-Pd NPs with *Shewanella oneidensis* MR-1 bacteria as a bio-electrochemical cell catalyts in pharmaceutical industry wastewater after 24 h catalytic degradation time, at 25°C, respectively.

Increasing DOX concentrations (5 mg/l, 15 mg/l, 30 mg/l and 45 mg/l) were operated during catalytic degradation process with bio-electrochemical cell assisted production of bio-Pd NPs with *Shewanella oneidensis* MR-1 bacteria as a bio-electrochemical cell catalyts in pharmaceutical industry wastewater, at pH=9.0, after 24 h catalytic degradation time, at 25°C, respectively (**Figure 13**). 86%, 95% and 78% DOX removal efficiencies were obtained to 5 mg/l, 15 mg/l and 45 mg/l DOX concentrations, respectively, at pH=9.0 and at 25°C (**Figure 13**). The maximum 99% DOX removal efficiency was found with catalytic degradation process in pharmaceutical industry wastewater, at 30 mg/l DOX, after 24 h catalytic degradation time, at pH=9.0 and at 25°C, respectively (**Figure 13**).

### 3.10. Effect of Increasing Bio-Pd NPs Concentrations for OFX and DOX Catalytic Removals with Bio-electrochemical Cell Assisted Production of Bio-Pd NPs with *Shewanella oneidensis* MR-1 Bacteria in Pharmaceutical Industry Wastewater

Increasing Bio-Pd NPs concentrations (5 mg/l, 10 mg/l, 20 mg/l, 30 mg/l, 40 mg/l and 60 mg/l) were operated during catalytic degradation process with bio-electrochemical cell assisted production of bio-Pd NPs with *Shewanella oneidensis* MR-1 bacteria as a bio-electrochemical cell catalyts in pharmaceutical industry wastewater, at 30 mg/l OFX, after 24 h catalytic degradation time, at pH=6.0, at 25°C, respectively (**Figure 14**). 53%, 67%, 74%, 86% and 91% OFX removal efficiencies were obtained to 5 mg/l, 10 mg/l, 20 mg/l, 30 mg/l and 60 mg/l Bio-Pd NPs concentrations, respectively, at 30 mg/l OFX, after 24 h catalytic degradation time, at pH=6.0, at 25°C, respectively (**Figure 14**). The maximum 99% OFX removal efficiency was measured to 40 mg/l Bio-Pd NPs with catalytic degradation process in pharmaceutical industry wastewater, at 30 mg/l OFX, after 24 h catalytic degradation time, at pH=6.0 and at 25°C, respectively (**Figure 14**).

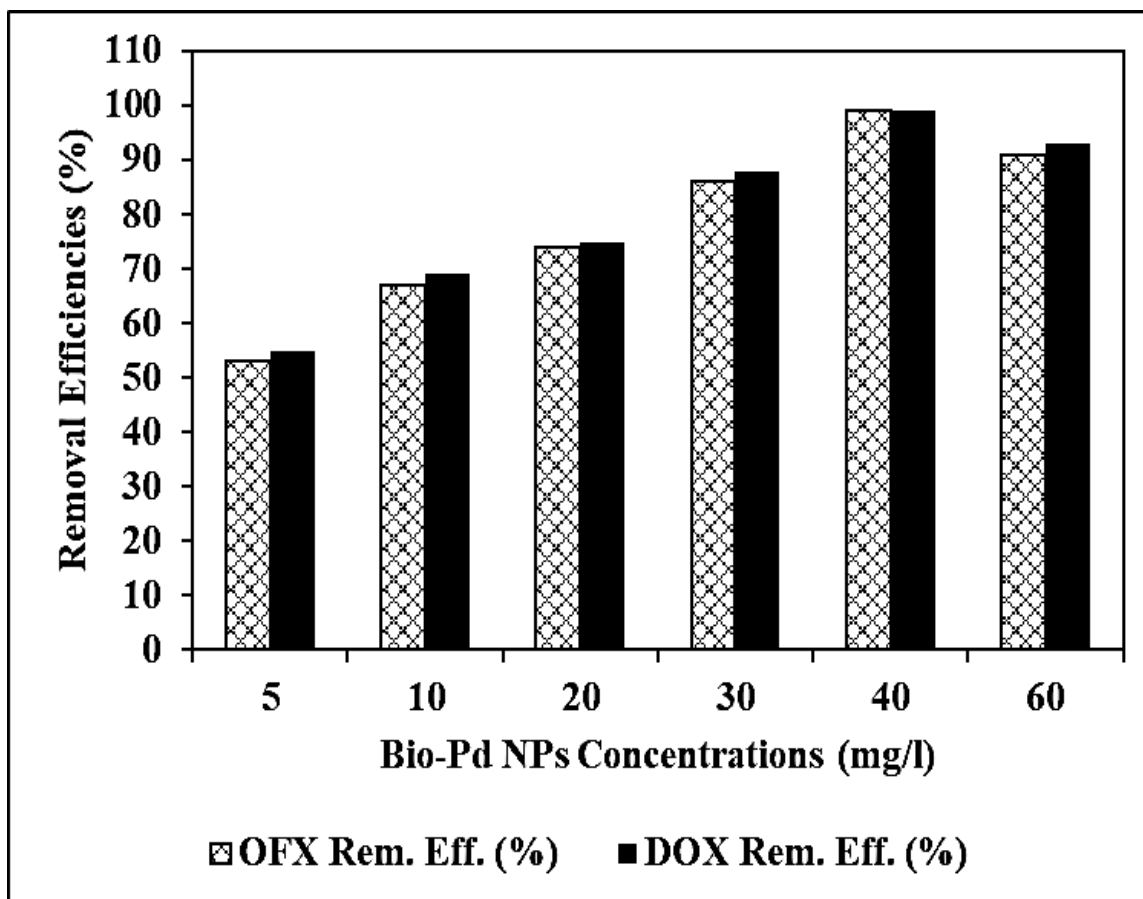


**Figure 14:** Effect of increasing Bio-Pd NPs concentrations for OFX and DOX catalytic removals with bio-electrochemical cell assisted production of bio-Pd NPs with *Shewanella oneidensis* MR-1 bacteria as a bio-electrochemical cell catalyts in pharmaceutical industry wastewater after 24 h catalytic degradation time, at 25°C, respectively.

Increasing Bio-Pd NPs concentrations (5 mg/l, 10 mg/l, 20 mg/l, 30 mg/l, 40 mg/l and 60 mg/l) were operated during catalytic degradation process with bio-electrochemical cell assisted production of bio-Pd NPs with *Shewanella oneidensis* MR-1 bacteria as a bio-electrochemical cell catalyts in pharmaceutical industry wastewater, at 30 mg/l DOX, after 24 h catalytic degradation time, at pH=9.0, at 25°C, respectively (**Figure 14**). 55%, 69%, 75%, 88% and 93% DOX removal efficiencies were obtained to 5 mg/l, 10 mg/l, 20 mg/l, 30 mg/l and 60 mg/l Bio-Pd NPs concentrations, respectively, at 30 mg/l DOX, after 24 h catalytic degradation time, at pH=9.0, at 25°C, respectively (**Figure 14**). The maximum 99% DOX removal efficiency was measured to 40 mg/l Bio-Pd NPs with catalytic degradation process in pharmaceutical industry wastewater, at 30 mg/l DOX, after 24 h catalytic degradation time, at pH=9.0 and at 25°C, respectively (**Figure 14**).

### 3.11. Effect of Different Bio-Pd NPs/Cell Dry Weight (CDW) Mass Ratios for OFX and DOX Catalytic Removals with Bio-electrochemical Cell Assisted Production of Bio-Pd NPs with

#### *Shewanella oneidensis* MR-1 Bacteria in Pharmaceutical Industry Wastewater

Different Bio-Pd NPs/CDW mass ratios (5/5wt, 6/4wt, 7/3wt, 8/2wt, 9/1wt, 1/9wt, 2/8wt, 3/7wt and 4/6wt, respectively) were examined during catalytic degradation process with bio-electrochemical cell assisted production of bio-Pd NPs with *Shewanella oneidensis* MR-1 bacteria as a bio-electrochemical cell catalyts in pharmaceutical industry wastewater, at 30 mg/l OFX, at 40 mg/l Bio-Pd NPs, after 24 h catalytic degradation time, at pH=6.0 and at 25°C, respectively (**Figure 15**). 79%, 83%, 76%, 61%, 47%, 54%, 63% and 77% OFX removal efficiencies were measured at 5/5wt, 7/3wt, 8/2wt, 9/1wt, 1/9wt, 2/8 wt, 3/7wt and 4/6wt Bio-Pd NPs/CDW mass ratios, respectively, at 30 mg/l OFX, after 24 h catalytic degradation time, at pH=6.0 and at 25°C, respectively (**Figure 15**). The maximum 99% OFX removal efficiency was measured at 6/4 wt Bio-Pd NPs/CDW mass ratios at 30 mg/l OFX, after 24 h catalytic degradation time, at pH=6.0 and at 25°C, respectively (**Figure 15**).

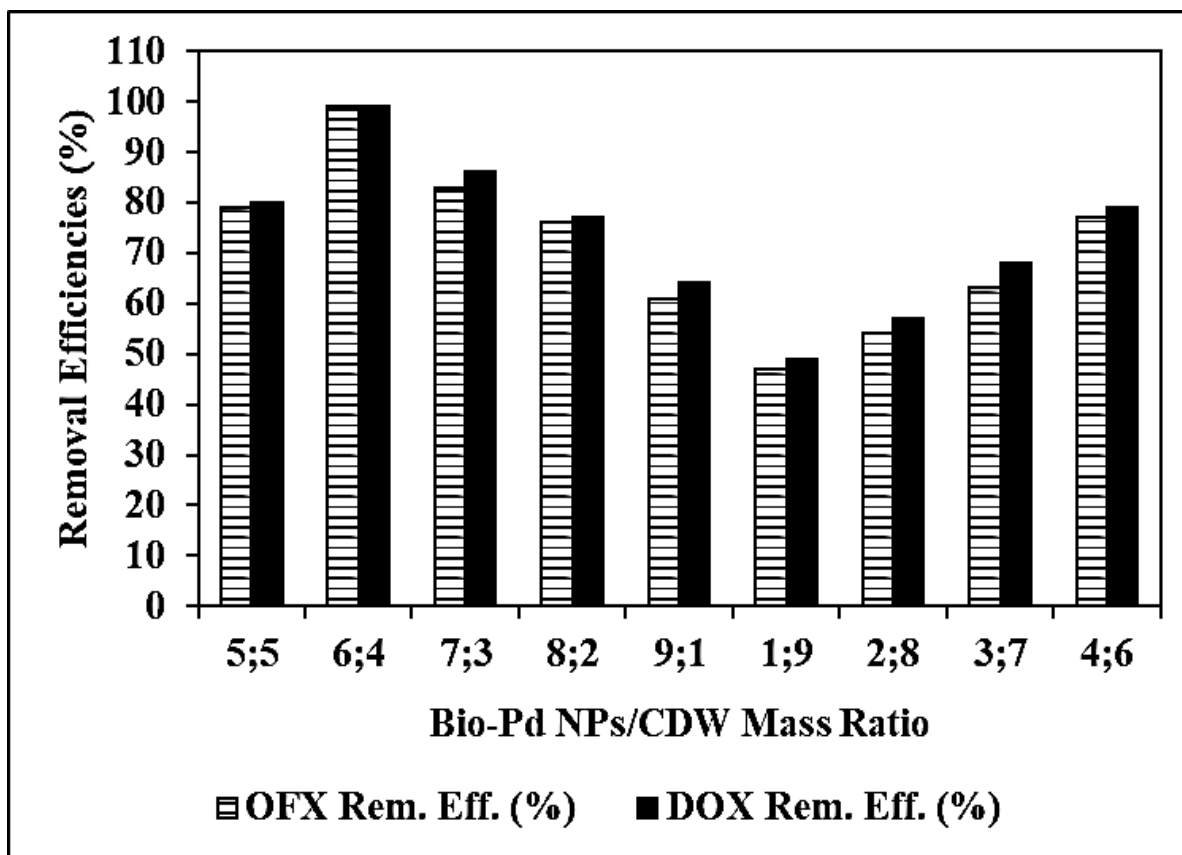


**Figure 15:** Effect of different Bio-Pd NPs/CDW mass ratios for OFX and DOX catalytic removals with bio-electrochemical cell assisted production of bio-Pd NPs with *Shewanella oneidensis* MR-1 bacteria as a bio-electrochemical cell catalysts in pharmaceutical industry wastewater after 24 h catalytic degradation time, at 25°C, respectively.

Different Bio-Pd NPs/CDW mass ratios (5/5wt, 6/4wt, 7/3wt, 8/2wt, 9/1wt, 1/9wt, 2/8wt, 3/7wt and 4/6wt, respectively) were examined during catalytic degradation process with bio-electrochemical cell assisted production of bio-Pd NPs with *Shewanella oneidensis* MR-1 bacteria as a bio-electrochemical cell catalysts in pharmaceutical industry wastewater, at 30 mg/l DOX, after 24 h catalytic degradation time, at pH=9.0 and at 25°C, respectively (**Figure 15**). 80%, 86%, 77%, 64%, 49%, 57%, 68% and 79% DOX removal efficiencies were measured at 5/5wt, 7/3wt, 8/2wt, 9/1wt, 1/9wt, 2/8wt, 3/7wt and 4/6wt Bio-Pd NPs/CDW mass ratios, respectively, at 30 mg/l DOX after 24 h catalytic degradation time, at pH=9.0 and at 25°C, respectively (**Figure 15**). The maximum 99% DOX removal efficiency was measured at 6/4wt Bio-Pd NPs/CDW mass ratios at 30 mg/l DOX, after 24 h catalytic degradation time, at pH=9.0 and at 25°C, respectively (**Figure 15**).

### 3.12. Effect of Different Recycle Times for OFX and DOX Catalytic Removals with Bio-electrochemical Cell Assisted Production of Bio-Pd NPs with *Shewanella oneidensis* MR-1 Bacteria in Pharmaceutical Industry Wastewater

Different recycle times (1., 2., 3., 4., 5., 6. and 7.) were operated for OFX catalytic removal with bio-electrochemical cell assisted production of bio-Pd NPs with *Shewanella oneidensis* MR-1 bacteria as a bio-electrochemical cell catalysts in pharmaceutical industry wastewater, at 30 mg/l OFX, 40 mg/l Bio-Pd NPs, at 6/4 wt Bio-Pd NPs/CDW mass ratio, after 24 h catalytic degradation time, at 25°C, respectively (**Figure 16**). 90%, 87%, 84%, 81%, 78%, 76% and 72% OFX removal efficiencies were measured after 2. recycle time, 3. recycle time, 4. recycle time, 5. recycle time, 6. recycle time and 7. recycle time, respectively, at 30 mg/l OFX, 40 mg/l Bio-Pd NPs, at 6/4wt Bio-Pd NPs/CDW mass ratio, after 24 h catalytic degradation time, at pH=6.0 and at 25°C, respectively (**Figure 16**). The maximum 99% OFX removal efficiency was measured in pharmaceutical industry wastewater during catalytic degradation process, after 1. recycle time, at 30 mg/l OFX, 40 mg/l Bio-Pd NPs, at 6/4wt Bio-Pd NPs/CDW mass ratio, after 24 h catalytic degradation time, at pH=6.0 and at 25°C, respectively (**Figure 16**).

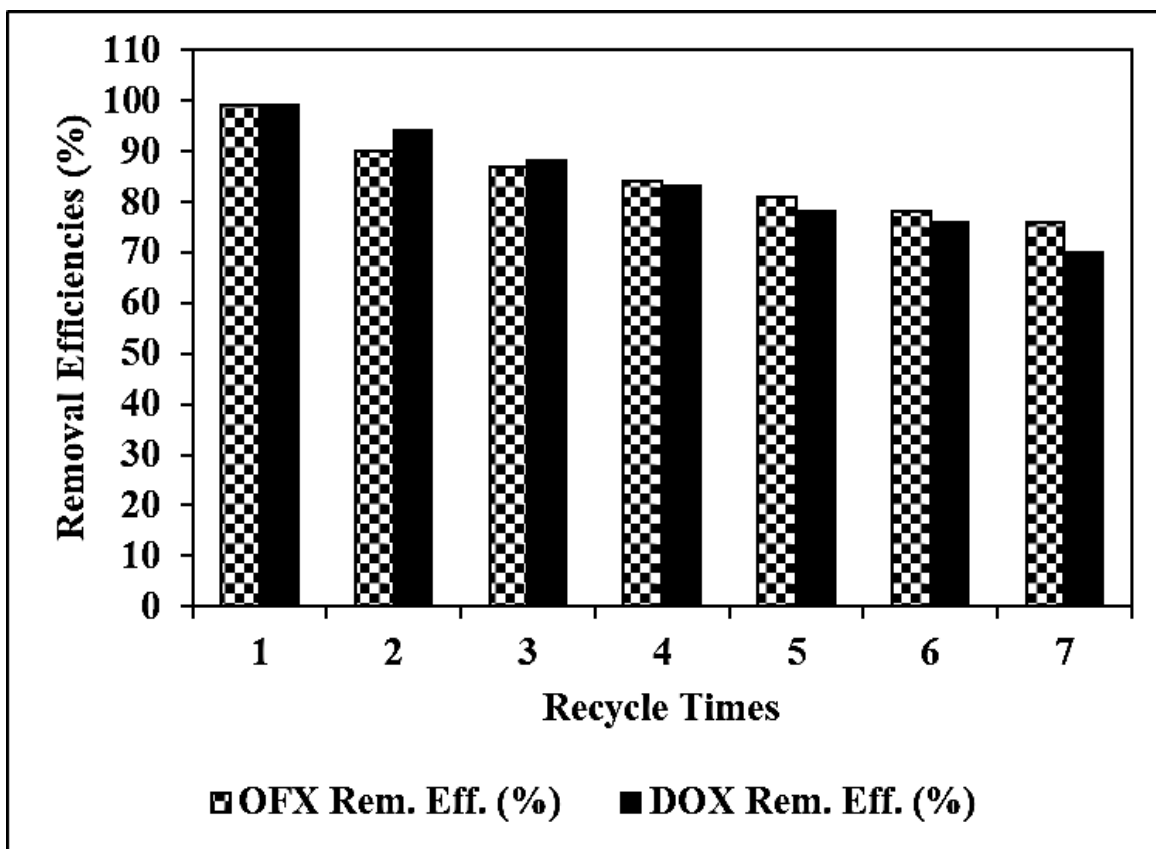


**Figure 16:** Effect of recycle times for OFX and DOX catalytic removals with bio-electrochemical cell assisted production of bio-Pd NPs with *Shewanella oneidensis* MR-1 bacteria as a bio-electrochemical cell catalysts in pharmaceutical industry wastewater after 24 h catalytic degradation time, at 25°C, respectively.

Different recycle times (1., 2., 3., 4., 5., 6. and 7.) were operated for DOX catalytic removal with bio-electrochemical cell assisted production of bio-Pd NPs with *Shewanella oneidensis* MR-1 bacteria as a bio-electrochemical cell catalysts in pharmaceutical industry wastewater, at 30 mg/l DOX, 40 mg/l Bio-Pd NPs, at 6/4wt Bio-Pd NPs/CDW mass ratio, after 24 h catalytic degradation time, at pH=9.0 and at 25°C, respectively (Figure 16). 94%, 88%, 83%, 78%, 76% and 70% DOX removal efficiencies were measured after 2. recycle time, 3. recycle time, 4. recycle time, 5. recycle time, 6. recycle time and 7. recycle time, respectively, at 30 mg/l DOX, 40 mg/l Bio-Pd NPs, at 6/4wt Bio-Pd NPs/CDW mass ratio, after 24 h catalytic degradation time, at pH=9.0 and at 25°C, respectively (Figure 16). The maximum 99% DOX removal efficiency was measured in pharmaceutical industry wastewater during

catalytic degradation process, after 1. recycle time, at 30 mg/l DOX, 40 mg/l Bio-Pd NPs, at 6/4wt Bio-Pd NPs/CDW mass ratio, after 24 h catalytic degradation time, at pH=9.0 and at 25°C, respectively (Figure 16).

### 3.13. The Comparison with other Scientific Studies in the Literature

Comparison of our study “Bio-electrochemical cell assisted production of biogenic palladium nanoparticles with *Shewanella oneidensis* MR-1 bacteria for the catalytic removal of ofloxacin (OFX) and doxycycline (DOX) micropollutants in pharmaceutical industry wastewaters” with other scientific studies in the literature is summarized at Table 2.

Micropollutants	Experimental Conditions and Results	References
Diclofenac	Continuous removal in MEC systems, with 57% lower removal efficiency	(De Gussemme et al., 2012)
Ciprofloxacin	According to Martins et al. (2017) was the removal negligible as 35 and 49% of ciprofloxacin was removed by active- and non-active catalyst, respectively	(He et al., 2020)
Sulfamethoxazole	85% Removal was accomplished after 24 h, with a removal rate of 0.110 1/h	(Martins et al., 2017)
Ibuprofen	No removal of the painkiller by bio-Pd produced by <i>D. vulgaris</i> ; however, it was removed by the bacterium	(Martins et al., 2017)
17 $\beta$ -estradiol	Low removal of the compound, 35 and 11%, by catalytic activity and adsorption, respectively	(Martins et al., 2017)

Ibuprofen, sulfamethoxazole, naproxen, furosemide, citalopram, diclofenac, atorvastatin, lorazepam	ibuprofen (69.5%) < sulfamethoxazole (80.6%) < naproxen (81.4%) < furosemide (89.7%) < citalopram (91.7%) < diclofenac (91.9%) < atorvastatin (> 94.3%) < lorazepam (97.2%).	(Law et al., 2023)
ciprofloxacin	the reductive removal of ciprofloxacin with Bio-Pd NPs catalyst, 87.70% ciprofloxacin removal at 25°C	He et al., 2020
Ofloxacin (OFX) and Doxycycline (DOX)	Bio-electrochemical cell assisted production of biogenic palladium nanoparticles with <i>Shewanella oneidensis</i> MR-1 bacteria for catalytic removal in pharmaceutical industry wastewater 99% OFX removal efficiency, at pH=6.0, after 24 h catalytic degradation time, at 30 mg/l OFX, 40 mg/l Bio-Pd NPs, Bio-Pd NPs/CDW mass ratio=6/4, at 25°C. 99% DOX removal efficiency, at pH=9.0, after 24 h catalytic degradation time, 30 mg/l DOX, 40 mg/l Bio-Pd NPs, Bio-Pd NPs/CDW mass ratio=6/4, at 25°C.	This study

**Table 2:** The Comparison with other Scientific Studies in the Literature

#### 4. Conclusions

The maximum 99% OFX removal efficiency was obtained catalytic removals with bio-electrochemical cell assisted production of bio-Pd NPs with *Shewanella oneidensis* MR-1 bacteria as a bio-electrochemical cell catalysts in pharmaceutical industry wastewater, at 30 mg/l OFX concentration, 40 mg/l Bio-Pd NPs concentration, Bio-Pd NPs/CDW mass ratio=6/4, after 24 h catalytic degradation time, at pH=6.0, at 25°C, respectively.

The maximum 99% DOX removal efficiency was observed catalytic removals with bio-electrochemical cell assisted production of bio-Pd NPs with *Shewanella oneidensis* MR-1 bacteria as a bio-electrochemical cell catalysts in pharmaceutical industry wastewater, at 30 mg/l DOX concentration, 40 mg/l Bio-Pd NPs concentration, Bio-Pd NPs/CDW mass ratio=6/4, after 24 h catalytic degradation time, at pH=9.0, at 25°C, respectively.

As a result, OFX and DOX micropollutants catalytic removals with bio-electrochemical cell assisted production of bio-Pd NPs with *Shewanella oneidensis* MR-1 bacteria as a heterostructure bio-electrochemical cell catalysts in pharmaceutical industry wastewater was stable in harsh environments such as acidic, alkaline, saline, and then was still effective process. When the amount of micropollutants was increased, the Bio-Pd NPs with *Shewanella oneidensis* MR-1 bacteria bio-electrochemical cell catalysts during catalytic degradation process performance was still considerable. The synthesis and optimization of Bio-Pd NPs with *Shewanella oneidensis* MR-1 bacteria heterostructure bio-electrochemical cell catalysts provides insights into the effects of preparation conditions on the material's characteristics and performance, as well as the application of the effectively designed bio-electrochemical cell catalyst in the removal of antibiotics, which can potentially be deployed for purifying wastewater, especially pharmaceutical industry wastewater.

In this study provides strong support for the use of Bio-Pd NPs with *Shewanella oneidensis* MR-1 bacteria bio-electrochemical cell catalysts with to efficiently remove micropollutants (OFX and DOX) from the environment and the possible applicability to wastewater treatment plants as a tertiary treatment system. In addition to, before applying Bio-Pd NPs with *Shewanella oneidensis* MR-1 bacteria bio-electrochemical cell catalysts in real wastewater treatment systems, more investigation is required. H<sub>2</sub>(g) can be submitted by implementing a bio-electrochemical cell system into the treatment plant or more research can be performed on finding an alternative electron donor for the reductive dehalogenation of halogenated micropollutants by the catalytic activity of the Bio-Pd NPs with *Shewanella oneidensis* MR-1 bacteria bio-electrochemical cell

catalysts. It is also important to recover Bio-Pd NPs with *Shewanella oneidensis* MR-1 bacteria bio-electrochemical cell catalysts for economical feasibility. The recovery of Pd<sup>+2</sup> ions from the supernatant solution, after production of Bio-Pd NPs with *Shewanella oneidensis* MR-1 bacteria bio-electrochemical cell catalysts, can be achieved by the addition of *Shewanella oneidensis* MR-1 to the solution, as the matrices of the cells and the supernatants are the same. It is also possible to recover leaching Pd NPs from the bio-Pd NPs, by chemical reaction, such as by the addition of nitric acid.

The catalytic removals with bio-electrochemical cell assisted production of bio-Pd NPs with *Shewanella oneidensis* MR-1 bacteria as a heterostructure bio-electrochemical cell catalysts method can also be applied to other waste metal ions to prepare the biogenic metals, facilitate their recovery and reuse in degrading micropollutants in pharmaceutical industry wastewater. Finally, the combination of a simple, easy operation preparation process, excellent performance and cost effective, makes this Bio-Pd NPs with *Shewanella oneidensis* MR-1 bacteria bio-electrochemical cell catalysts a promising option during catalytic degradation process in pharmaceutical industry wastewater treatment.

#### Acknowledgement

This research study was undertaken in the Environmental Microbiology Laboratories at Dokuz Eylül University Engineering Faculty Environmental Engineering Department, Izmir, Turkey. The authors would like to thank this body for providing financial support.

#### References

1. Abdalla, A.M., Hossain, S., Nisfindy, O.B., Azad, A.T., Dawood, M., Azad, A.K. (2018). Hydrogen production, storage, transportation and key challenges with applications: A review. *Energy Convers. Manag.*, 165:602–627.
2. Abtahi, S.M., Ilyas, S., Joannis Cassan, C., Albasi, C., de Vos, W.M. (2018). Micropollutants removal from secondary-treated municipal wastewater using weak polyelectrolyte multilayer based nanofiltration membranes. *J. Membr. Sci.*, 548:654-666.
3. Adams, C., Wang, Y., Loftin, K., Meyer, M. (2002). Removal of antibiotics from surface and distilled water in conventional water treatment processes. *J. Environ. Eng.*, 128:253-260.
4. Adams, C.P., Walker, K.A., Obare, S.O., Docherty, K.M. (2014). Size-dependent antimicrobial effects of novel palladium nanoparticles. *PLoS One.*, 9(1):e85981.
5. Ahring, B.K., Schmidt, J.E., Winther-Nielsen, M., Macario, A.J., Conway de Macario, E. (1993). Effect of medium

- composition and sludge removal on the production, composition, and architecture of thermophilic (55 degrees C) acetate-utilizing granules from an upflow anaerobic sludge blanket reactor. *Appl. Environ. Microbiol.*, 59(8):2538–2345.
6. Aki, H., Murata, A., Yamamoto, S., Kondoh, J., Maeda, T., et al. (2005). Penetration of residential fuel cells and CO mitigation—case studies in Japan by multi-objective models. *Int. J. Hydrog. Energy.*, 30(9):943–952.
  7. Akyon, B., McLaughlin, M., Hernández, F., Blotevogel, J., Bibby, K. Characterization and biological removal of organic compounds from hydraulic fracturing produced water. *Environ. Sci. Process.*, 2019;21:279-290.
  8. Alagha, O., Ouerfelli, N., Kochkar, H., Almessiere, M.A., Slimani, Y., Manikandan, A., Baykal, A., Mostafa, A., Zubair, M., Barghouthi, M.H. Kinetic modeling for photo-assisted penicillin G degradation of (Mn<sub>0.5</sub>Zn<sub>0.5</sub>)[CdxFe<sub>2-x</sub>]O<sub>4</sub> (x ≤ 0.05) nanospinel ferrites. *Nanomaterials*, 2021;11:970-986.
  9. Al-Hamadani, Y.A.J., K.H. Chu, J.R.V. Flora, D.-H. Kim, M. Jang, J. Sohn, W. Joo, Y. Yoon, Sonocatalytic degradation enhancement for ibuprofen and sulfamethoxazole in the presence of glass beads and single-walled carbon nanotubes. *Ultrason. Sonochem.*, 2016;32:440–448.
  10. Alibhai, K.R.K., Mehrotra, I., Forster, C.F. Heavy-metal binding to digested-sludge. *Water Res.*, 1985;19(12):1483–1488.
  11. Allen, R.M., Bennetto, H.P. Microbial fuel-cells – electricity production from carbohydrates. *Appl Biochem Biotechnol.* 1993;39(1):27–40.
  12. Alygizakis, N.A., Gago-Ferrero, P., Borova, V.L., Pavlidou, A., Hatzianestis, I., Thomaidis, N.S. Occurrence and spatial distribution of 158 pharmaceuticals, drugs of abuse and related metabolites in offshore seawater. *Sci. Total Environ.*, 2016;541:1097-1105.
  13. Amini, Z., Givianrad, M.H., Husain, S.W., Azar, P.A., Saber-Tehrani, M. Cu-S codoping TiO<sub>2</sub>/SiO<sub>2</sub> and TiO<sub>2</sub>/SiO<sub>2</sub>/Fe<sub>3</sub>O<sub>4</sub> core-shell nanocomposites as a novel purple LED illumination active photocatalyst for degradation of diclofenac: the effect of different scavenger agents and optimization. *Chem. Eng. Commun.*, 2020;207:1536-1553.
  14. Andriole, V.T. (1989). The Quinolones, *Academic Press*,
  15. Anjali, R., Shanthakumar, S. Insights on the current status of occurrence and removal of antibiotics in wastewater by advanced oxidation processes. *J. Environ. Manage.*, 2019;246:51-62.
  16. Antonelli, R., Malpass, G.R.P., da Silva, M.G.C., Vieira, M.G.A. Adsorption of ciprofloxacin onto thermally modified bentonite clay: Experimental design, characterization, and adsorbent regeneration. *J. Environ. Chem. Eng.* 2020;8:104553.
  17. Appels, L., Baeyens, J., Degrève, J., Dewil, R. Principles and potential of the anaerobic digestion of waste-activated sludge. *Prog. Energy Combust. Sci.* 2008;34(6):755–781.
  18. Arenas, N.E., Melo, V.M. Producción pecuaria y emergencia de antibiótico resistencia en Colombia: Revisión sistemática. *Infectio*, 2018;22:110-119.
  19. Babaei, A.A., Golshan, M., Kakavandi, B. A heterogeneous photocatalytic sulfate radical-based oxidation process for efficient degradation of 4-chlorophenol using TiO<sub>2</sub> anchored on Fe oxides@ carbon, *Process Saf. Environ. Protection.*, 2021;149:35-47.
  20. Baird, R.B., Eaton, A.D., Rice, E.W. Standard Methods for the Examination of Water and Wastewater. 23rd. Edition, Rice, E.W. (editors), American Public Health Association (APHA), American Water Works Association (AWWA), Water Environment Federation (WEF). American Public Health Association 800 I Street, NW Washington DC: 20001-3770, USA, January 1, 2017; ISBN-13: 978-0875532875; ISBN-10: 087553287X.
  21. Bali, R., Razak, N., Lumb, A., Harris, A.T. The synthesis of metallic nanoparticles inside live plants. International Conference on Nanoscience and Nanotechnology, 2006. INSPEC Accession Number:9562234, doi:10.1109/ICNN.2006.340592.
  22. Bansal, P., Verma, A., Aggarwal, K., Singh, A., Gupta, S. Investigations on the degradation of an antibiotic Cephalexin using suspended and supported TiO<sub>2</sub>: Mineralization and durability studies. *The Canad. J. Chem. Eng.*, 2016;94:1269-1276.
  23. Barry, S. Dangerously high levels of antibiotics found in world's major rivers, says study. *World news global study*, Euronews, 2019;1:1-10.
  24. Berg, J.M., Romoser, A., Banerjee, N., Zebda, R., Sayes, C.M. The relationship between pH and zeta potential of similar to 30 nm metal oxide nanoparticle suspensions relevant to in vitro toxicological evaluations. *Nanotoxicology.*, 2009;3(4):276–283.
  25. Bobu, M., Yediler, A., Siminiceanu, I., Zhang, F., Schulte-Hostede, S. Comparison of different advanced oxidation processes for the degradation of two fluoroquinolone antibiotics in aqueous solutions. *J. Environ. Sci. Health. Toxic/hazardous Substance Environ. Eng.*, 2013;48:251-262.
  26. Bucking, C., Piepenbrock, A., Kappler, A., Gescher, J. Outermembrane cytochrome-independent reduction of extracellular electron acceptors in *Shewanella oneidensis*. *Microbiology (Read)*, 2012;158(Pt 8):2144–2157.
  27. Casanova, L.M., Sobsey, M.D. Antibiotic-resistant enteric bacteria in environmental waters. *Water*, 2016;8(12):561-567.
  28. Chaturvedi, V., Verma, P. Microbial fuel cell: A green approach for the utilization of waste for the generation of bioelectricity. *Bioresour. Bioprocess.* 2016;3(1):Article number:38.
  29. Chen, Y., Chen, Y. Difference in toxicity of Pd (II) and mechanism of action before and after reduction by *Bacillus wiedmannii* MSM. *Environ Sci Pollut Res.*, 2021;29:1824–1835.
  30. Cheng, H.Y., Hou, Y.N., Zhang, X., Yang, Z.N., Xu, T., Wang, A.J. Activating electrochemical catalytic activity of bio-palladium by hybridizing with carbon nanotube as “e(-) Bridge”. *Sci. Rep.*, 2017;7(1):16588.
  31. Courtney, J., Deplanche, K., Rees, N.V., Macaskie, L.E. Biomanufacture of nano-Pd(0) by *Escherichia coli* and electrochemical activity of bio-Pd(0) made at the expense of H<sub>2</sub> and formate as electron donors. *Biotechnol. Lett.*, 2016;38(11):1903–1910.
  32. Coy, E., Siuzdak, K., Pavlenko, M., Załęski, K., Graniel, O., Ziółek, M., Sebastian Balme, S., Miele, P., Weber, M., Bechelany, M., Iatsunskyi, I. Enhancing photocatalytic performance and solar absorption by schottky nanodiodes heterojunctions in mechanically resilient palladium coated TiO<sub>2</sub>/Si nanopillars by atomic layer deposition. *Chem. Eng. J.*, 2020;392:123702.
  33. de Andrade, J.R., Oliveira, M.F., da Silva, M.G.C., Vieira, M.G.A. Adsorption of pharmaceuticals from water and wastewater using nonconventional low-cost materials: a review. *Ind. Eng. Chem. Res.*, 2018;57:3103-3127.
  34. De Corte, S., Hennebel, T., De Gussemme, B., Verstraete, W., Boon, N. Bio-palladium: from metal recovery to catalytic applications. *Microb Biotechnol.*, 2012;5(1):5–17.
  35. De Corte, S., Hennebel, T., Fitts, J.P., Sabbe, T., Bliznuk, V., Verschuere, S., van der Lelie, D., Verstraete, W., Boon, N. Biosupported bimetallic Pd-Au nanocatalysts for

- dechlorination of environmental contaminants. *Env. Sci. Technol.*, 2011;45(19):8506–8513.
36. De Gussemme, B., Hennebel, T., Vanhaecke, L., Soetaert, M., Desloover, J., Wille, K., Verbeke, K., Verstraete, W., Boon, N. Biogenic palladium enhances diatrizoate removal from hospital wastewater in a microbial electrolysis cell. *Env. Sci. Technol.*, 2011;45(13):5737–5745.
  37. De Gussemme, B., Soetaert, M., Hennebel, T., Vanhaecke, L., Boon, N., Verstraete, W. Catalytic dechlorination of diclofenac by biogenic palladium in a microbial electrolysis cell. *Microb. Biotechnol.*, 2012;5(3):396–402.
  38. de Souza Santos, L.V., Meireles, A.M., Lange, L.C. Degradation of antibiotics norfloxacin by fenton, UV and UV/H<sub>2</sub>O<sub>2</sub>. *J. Environ. Manag.*, 2015;154:8-12.
  39. De Windt, W., Aelterman, P., Verstraete, W. Bioreductive deposition of palladium (0) nanoparticles on *Shewanella oneidensis* with catalytic activity towards reductive dechlorination of polychlorinated biphenyls. *Env. Microbiol.*, 2005;7(3):314–325.
  40. De Windt, W., Boon, N., Van den Bulcke, J., Rubberecht, L., Prata, F., Mast, J., Hennebel, T., Verstraete, W. Biological control of the size and reactivity of catalytic Pd(0) produced by *Shewanella oneidensis*. *Antonie van Leeuwenhoek*. 2006;90(4):377–389.
  41. Dekura, S., Kobayashi, H., Kusada, K., Kitagawa, H. Hydrogen in palladium and storage properties of related nanomaterials: Size, shape, alloying, and metal-organic framework coating effects. *Chemphyschem.*, 2019;20(10):1158–1176.
  42. Deplanche, K., Bennett, J.A., Mikheenko, I.P., Omajali, J., Wells, A.S., Meadows, R.E., Wood, J., Macaskie, L.E. Catalytic activity of biomass-supported Pd nanoparticles: Influence of the biological component in catalytic efficacy and potential application in ‘green’ synthesis of fine chemicals and pharmaceuticals. *Appl. Catal. B: Environ.*, 2014;147:651-665.
  43. Deplanche, K., Caldelari, I., Mikheenko, I.P., Sargent, F., Macaskie, L.E. Involvement of hydrogenases in the formation of highly catalytic Pd(0) nanoparticles by bioreduction of Pd (II) using *Escherichia coli* mutant strains. *Microbiology.*, 2010;156(9):2630–2640.
  44. Dinh, Q.T., Moreau-Guigon, E., Labadie, P., Alliot, F., Teil, M.-J., Blanchard, M., Chevreuil, M. Occurrence of antibiotics in rural catchments. *Chemosphere*, 2017;168:483-490.
  45. Dong, D., Zhang, L., Liu, S., Guo, Z., Hua, X. Antibiotics in water and sediments from Liao River in Jilin Province, China: occurrence, distribution, and risk assessment. *Environ. Earth Sci.*, 2016;75(16):1202, ref.45.
  46. Dundas, C.M., Graham, A.J., Romanovicz, D.K., Keitz, B.K. Extracellular electron transfer by *shewanella oneidensis* controls palladium nanoparticle phenotype. *ACS Synth. Biol.* 2018;7(12):2726–2736.
  47. Eckenfelder, W.W., *Industrial Water Pollution Control* (2nd ed), Signapore: McGraw-Hill Inc.,1989.
  48. Eddy, D.R., Puri, F.N., Noviyanti, A.R. Synthesis and photocatalytic activity of silica-based sand quartz as the supporting TiO<sub>2</sub> photocatalyst. *Proced. Chem.*, 2015;17:55-58.
  49. Ehrl, B.N., Kundu, K., Gharasoo, M., Marozava, S., Elsner, M. Rate-limiting mass transfer in micropollutant degradation revealed by isotope fractionation in chemostat. *Env. Sci. Technol.*, 2019;53(3):1197–1205.
  50. Espino-López, I.E., Romero-Romo, M., Montes de Oca-Yemha, M.G., Morales-Gil, P., Ramírez-Silva, M.T., Mostany, J., Palomar-Pardave, M. Palladium nanoparticles electrodeposition onto glassy carbon from a deep eutectic solvent at 298 K and their catalytic performance toward formic acid oxidation. *J Electrochem Soc.* 2018;166(1):D3205–3211.
  51. Fahmy, K., Merroun, M., Pollmann, K., Raff, J., Savchuk, O., Hennig, C., Selenska-Pobell, S. Secondary structure and Pd(II) coordination in S-layer proteins from *Bacillus sphaericus* studied by infrared and X-ray absorption spectroscopy. *Biophys J.*, 2006;91(3):996–1007.
  52. Fahmy, S.A., Preis, E., Bakowsky, U., El-Said Azzazy, H.M. Palladium nanoparticles fabricated by green chemistry: Promising chemotherapeutic, antioxidant and antimicrobial agents. *Materials.*, 2020;13(17):3661-3683.
  53. Fekadu, S., Alemayehu, E., Dewil, R., Van der Bruggen, B. Pharmaceuticals in freshwater aquatic environments: a comparison of the african and european challenge. *Sci. Total Environ.*, 2019;654:324-337.
  54. Feng, S., Ngo, H.H., Guo, W., Chang, S.W., Nguyen, D.D., Cheng, D., Varjani, S., Lei, Z., Liu, Y. Roles and applications of enzymes for resistant pollutants removal in wastewater treatment. *Bioresour Technol.*, 2021;335:125278.
  55. Ferri, M., Ranucci, E., Romagnoli, P., Giaccone, V. Antimicrobial resistance: A global emerging threat to public health systems. *Crit. Rev. Food Sci.*, 2017;57:2857-2876.
  56. Folens, K., Van Hulle, S., Vanhaecke, F., Du Laing, G. Chemical fractionation and speciation modelling for optimization of ion-exchange processes to recover palladium from industrial wastewater. *Water Sci. Technol.*, 2016;73:1738-1745.
  57. Forrez, I., Carballa, M., Fink, G., Wick, A., Hennebel, T., Vanhaecke, L., Ternes, T., Boon, N., Verstraete, W. Biogenic metals for the oxidative and reductive removal of pharmaceuticals, biocides and iodinated contrast media in a polishing membrane bioreactor. *Water Res.*, 2011;45(4):1763-1773.
  58. Franke-Whittle, I.H., Walter, A., Ebner, C., Insam, H. Investigation into the effect of high concentrations of volatile fatty acids in anaerobic digestion on methanogenic communities. *Waste Manag.*, 2014;34(11):2080–2089.
  59. Fredrickson, J.K., Romine, M.F., Beliaev, A.S., Auchtung, J.M., Driscoll, M.E., Gardner, T.S., Neelson, K.H., Osterman, A.L., Pinchuk, G., L Reed, J.L., Rodionov, D.A., Rodrigues, J.L.M., Saffarini, D.A., Serres, M.H., Spormann, A.M., Zhulin, I.B., Tiedje, J.M. Towards environmental systems biology of *Shewanella*. *Nat. Rev. Microbiol.*, 2008;6(8):592–603.
  60. Fridkin, S., Baggs, J., Fagan, R., Magill, S., Pollack, L.A., Malpiedi, P., Slayton, R., Khader, K., Rubin, M.A., Jones, M., Samore, M.H., Dumyati, G., Dodds-Ashley, E., Meek, J., Yousey-Hindes, K., Jernigan, J., Shehab, N., Herrera, R., McDonald, C.L., Schneider, A., Srinivasan, A. Vital signs: improving antibiotic use among hospitalized patients. *MMWR-Morb. Mortal. Wkly. Rep.*, 2014;63(9):194-200.
  61. Garg, A., Sangal, V.K., Bajpai, P.K. Decolorization and degradation of Reactive Black 5 dye by photocatalysis: Modeling, optimization and kinetic study, *Desalin. Water Treat.* 2016;57:18003-180015.
  62. Gomez-Bolivar, J., Mikheenko, I.P., Macaskie, L.E., Merroun, M.L. Characterization of palladium nanoparticles produced by healthy and microwave-injured cells of *desulfovibrio desulfuricans* and *escherichia coli*. *Nanomaterials (Basel).*, 2019a;9(6):857.
  63. Gomez-Bolivar, J., Mikheenko, I.P., Orozco, R.L., Sharma, S., Banerjee, D., Walker M, Hand, L.A., Merroun, M.L., Macaskie, L.E. Synthesis of Pd/Ru bimetallic nanoparticles by *Escherichia coli* and potential as a catalyst for upgrading 5-hydroxymethyl furfural into liquid fuel precursors. *Front Microbiol.* 2019b;10:1276.

64. Gould, M.S., Genetelli, E.J. Heavy-metal complexation behavior in anaerobically digested sludges. *Water Res.* 1978;12(8):505–512.
65. Guo, S., Zhang, S., Su, D., Sun, S. Seed-mediated synthesis of core/shell FePtM/FePt (M = Pd, Au) nanowires and their electrocatalysis for oxygen reduction reaction. *J. Am. Chem. Soc.*, 2013;135(37):13879–13884.
66. Hazarika, M., Borah, D., Bora, P., Silva, A.R., Das, P. Biogenic synthesis of palladium nanoparticles and their applications as catalyst and antimicrobial agent. *PLoS One.*, 2017;12(9):e0184936.
67. He, P., Mao, T., Wang, A., Yin, Y., Shen, J., Chen, H., Zhang, P. Enhanced reductive removal of ciprofloxacin in pharmaceutical wastewater using biogenic palladium nanoparticles by bubbling H<sub>2</sub>. *Royal Society of Chemistry, RSC Adv.* 2020;10(44):26067–26077.
68. Hennebel, T., De Corte, S., Vanhaecke, L., Vanherck, K., Forrez, I., De Gussemme, B., Verhagen, P., Verbeken, K., Van der Bruggen, B., Vankelecom, I., Boon, N., Verstraete, W. Removal of diatrizoate with catalytically active membranes incorporating microbially produced palladium nanoparticles. *Water Res.*, 2010;44(5):1498–1506.
69. Hennebel, T., De Gussemme, B., Boon, N., Verstraete, W. Biogenic metals in advanced water treatment. *Trends Biotechnol.*, 2009a;27(2):90–98.
70. Hennebel, T., Simoen, H., De Windt, W., Verloo, M., Boon, N., Verstraete, W. Biocatalytic dechlorination of trichloroethylene with bio-palladium in a pilot-scale membrane reactor. *Biotechnol Bioeng.*, 2009b;102(4):995–1002.
71. Hennebel, T., Van Nevel, S., Verschuere, S., De Corte, S., De Gussemme, B., Cuvelier, C., Fitts, J.P., van der Lelie, D., Boon, N., Verstraete, W. Palladium nanoparticles produced by fermentatively cultivated bacteria as catalyst for diatrizoate removal with biogenic hydrogen. *Appl. Microbiol. Biotechnol.* 2011;91(5):1435–1445
72. Hoffmann, J.E. Recovery of platinum-group metals from gabbroic rocks metals from auto catalysts. *Jom.*, 2012;40(6):40–44.
73. Hou, Y.-N., Liu, H., Han, J.-L., Cai, W.-W., Zhou, J., Wang, A.-J., Cheng, H.-Y. Electroactive biofilm serving as the green synthesizer and stabilizer for in situ fabricating 3D nanopalladium network: An efficient electrocatalyst. *ACS Sustainable Chem. Eng.*, 2016;4:5392–5397.
74. Hou, Y.-N., Sun, S.-Y., Yang, Z.-N., Yun, H., Zhu, T.-T., Ma, J.-F., Han, J.-L., Wang, A.-J., Cheng, H.-Y. *Shewanella oneidensis* MR-1 self-assembled Pd-cells-rGO conductive composite for enhancing electrocatalysis. *Environ Res.* 2020;184:109317.
75. Hou, Y.-N., Zhang, B., Yun, H., Yang, Z.-N., Han, J.-L., Zhou, J., Wang, A.-J., Cheng, H.-Y. Palladized cells as suspension catalyst and electrochemical catalyst for reductively degrading aromatics contaminants: Roles of Pd size and distribution. *Water Res.*, 2017;125:288–297.
76. Hulshoff Pol, L.W., de Castro Lopes, S.I., Lettinga, G., Lens, P.N. Anaerobic sludge granulation. *Water Res.*, 2004;38(6):1376–1389.
77. Huo, T.I. The first case of multidrug-resistant NDM-1-harboring Enterobacteriaceae in Taiwan: here comes the superbacteria! *J. Chin. Med. Assoc.*, 2010;73:557–558.
78. Idham, M.F., Abdullah, B., Yusof, K.M. Effects of two cycle heat treatment on the microstructure and hardness of ductile iron. *Pertanika. J. Sci. Technol.*, 2017;25:99–106.
79. Idham, M.F., Falyouna, O., Eljamal, O. Effect of graphene oxide synthesis method on the adsorption performance of pharmaceutical contaminants. *Proc. Int. Exch. Innov. Conf. Eng. Sci.*, 2021;7:232–239.
80. Ji, Z., Zhang, H., Liu, H., Yaghi, O.M., Yang, P. Cytoprotective metalorganic frameworks for anaerobic bacteria. *Proc. Natl. Acad. Sci.*, 2018;115(42):10582–10587.
81. Jiménez-Tototzintle, M., Ferreira, I.J., da Silva Duque, S., Guimarães Barrocas, P.R., Saggiaro, E.M. Removal of contaminants of emerging concern (CECs) and antibiotic resistant bacteria in urban wastewater using UVA/TiO<sub>2</sub>/H<sub>2</sub>O<sub>2</sub> photocatalysis. *Chemosphere*, 2018;210:449–457.
82. Johnson, J. R., Murray, A.C., Gajewski, A., Sullivan, M., Snippes, P., Kuskowski, M.A., Smith, K.E. Isolation and molecular characterization of nalidixic acid-resistant extraintestinal pathogenic *Escherichia coli* from retail chicken products. *Antimicrob. Agents. Chemother.*, 2003;47(7):2161–2168.
83. Joudeh, N., Saragliadis, A., Schulz, C., Voigt, A., Almaas, E., Linke, D. Transcriptomic response analysis of *Escherichia coli* to palladium stress. *Front Microbiol.*, 2021;12:2840.
84. Karthikeyan, K.G., Meyer, M.T. Occurrence of antibiotics in wastewater treatment facilities in Wisconsin, USA., *Sci. Total Environ.*, 2006;361:196–207.
85. Kerrigan, J.F., Sandberg, K.D., Engstrom, D.R., LaPara, T.M., Arnold, W.A. Small and large-scale distribution of four classes of antibiotics in sediment: association with metals and antibiotic resistance genes. *Environ. Sci. Process. Impacts.*, 2018;20:1167–1179.
86. Kritas, S., Ronconi, G., Caraffa, A., Gallenga, C., Ross, R., Conti, P. Mast cells contribute to coronavirus-induced inflammation: new anti-inflammatory strategy. *J. Biol. Regul. Homeost. Agents.*, 2020;34:9–14.
87. Kumar, R., Singh, L., Zularisam, A.W. Exoelectrogens: Recent advances in molecular drivers involved in extracellular electron transfer and strategies used to improve it for microbial fuel cell applications. *Renew Sustain Energy Rev.*, 2016;56:1322–1336.
88. Kumari, S., Tyagi, M., Jagadevan, S. Mechanistic removal of environmental contaminants using biogenic nano-materials. *Int J Environ Sci Technol.*, 2019;16(11):7591–7606.
89. Kundu, K., Marozava, S., Ehrh, B., Merl-Pham, J., Griebler, C., Elsner, M. Defining lower limits of biodegradation: atrazine degradation regulated by mass transfer and maintenance demand in *Arthrobacter aureus* TC1. *ISME J.*, 2019;13(9):2236–2251.
90. Law, C.K.Y., Kundu, K., Bonin, L., Peñacoba-Antona, L., Bolea-Fernandez, E., Vanhaecke, F., Rabaey, K., Esteve-Núñez, A., De Gussemme, B., Boon, N. Electrochemically assisted production of biogenic palladium nanoparticles for the catalytic removal of micropollutants in wastewater treatment plants effluent. *Journal of Environmental Sciences*, 2023;128:203–212.
91. Leso, V., Iavicoli, I. Palladium nanoparticles: Toxicological effects and potential implications for occupational risk assessment. *Int J Mol Sci.*, 2018;19(2):503.
92. Linares-Solano, A., Lillo-Ródenas, M., Marco-Lozar, J., Kunowsky, M., Romero-Anaya, A. NaOH and KOH for preparing activated carbons used in energy and environmental applications. *Int. J. Energy Environ. Econ.*, 2012;20:59–91.
93. Liu, J., Zheng, Y., Hong, Z., Cai, K., Zhao, F., Han, H. Microbial synthesis of highly dispersed PdAu alloy for enhanced electrocatalysis. *Sci Adv.*, 2016;2(9):e1600858
94. Lloyd, J.R., Yong, P., Macaskie, L.E. Enzymatic recovery of elemental palladium by using sulfate-reducing bacteria. *Appl. Env. Microbiol.*, 1998;64(11):4607–4609.
95. Lovley, D.R. Dissimilatory metal reduction. *Annu Rev Microbiol.*, 1993;47:263–290.

96. Lovley, D.R. The microbe electric: conversion of organic matter to electricity. *Curr. Opin. Biotechnol.*, 2008;19(6):564–571.
97. Makarov, V.V., Love, A.J., Sinitsyna, O.V., Makarova, S.S., Yaminsky, I.V., Taliansky, M.E., Kalinina, N.O. “Green” nanotechnologies: synthesis of metal nanoparticles using plants. *Acta Nat.*, 2014;6(1):35–44.
98. Marshall, M.J., Beliaev, A.S., Dohnalkova, A.C., Kennedy, D.W., Shi, L., Wang, Z., Boyanov, M.I., Lai, B., Kemner, K.M., McLean, J.S., Reed, S.B., Culley, D.E., Bailey, V.L., Simonson, C.J., Saffarini, D.A., Romine, M.F., Zachara, J.M., James K Fredrickson, J.K. c-Type cytochrome-dependent formation of U (IV) nanoparticles by *Shewanella oneidensis*. *PLoS Biol.*, 2006;4(9):e268.
99. Martins, M., Mourato, C., Sanches, S., Noronha, J.P., Crespo, M.T.B., Pereira, I.A.C. Biogenic platinum and palladium nanoparticles as new catalysts for the removal of pharmaceutical compounds. *Water Res.*, 2017;108:160–168.
100. Matsena, M.T., Tichapondwa, S.M., Chirwa, E.M.N. Synthesis of biogenic palladium nanoparticles using *Citrobacter* sp. for application as anode electrocatalyst in a microbial fuel cell. *Catalysts.*, 2020;10(8):838.
101. Maycock, D.S., Watts, C.D. Pharmaceuticals in drinking water. *Encycl. Environ. Heal.*, 2011;472–484.
102. McConnell, M.M., Truelstrup Hansen, L., Jamieson, R.C., Neudorf, K.D., Yost, C.K., Tong, A. Removal of antibiotic resistance genes in two tertiary level municipal wastewater treatment plants. *Sci. Total Environ.*, 2018;643:292–300.
103. Md Ishak, N.A.I., Kamarudin, S.K., Timmiati, S.N. Green synthesis of metal and metal oxide nanoparticles via plant extracts: an overview. *Mater. Res. Exp.*, 2019;6(11):112004.
104. Miao, D., Peng, J., Wang, M., Shao, S., Wang, L., Gao, S. Removal of atorvastatin in water mediated by  $\text{CuFe}_2\text{O}_4$  activated peroxymonosulfate. *Chem. Eng. J.*, 2018;346:1–10.
105. Mikheenko, I.P., Rousset, M., Dementin, S., Macaskie, L.E. Bioaccumulation of palladium by *Desulfovibrio fructosivorans* wild-type and hydrogenase-deficient strains. *Appl. Env. Microbiol.*, 2008;74(19):6144–6146.
106. Monteagudo, J.M., El-taliawy, H., Duran, A., Caro, G., Bester, K. Sono-activated persulfate oxidation of diclofenac: degradation, kinetics, pathway and contribution of the different radicals involved. *J. Hazard. Mater.*, 2018;357:457–465.
107. Mughal, B., Zaidi, S., Zhang, X., Hassan, S.U. Biogenic nanoparticles: Synthesis, characterisation and applications. *Appl Sci.*, 2021;11:2598.
108. Ng, C.K., Cai Tan, T.K., Song, H., Cao, B. Reductive formation of palladium nanoparticles by *Shewanella oneidensis*: role of outer membrane cytochromes and hydrogenases. *RSC Adv.*, 2013a;3(44):22498–22503.
109. Ng, C.K., Sivakumar, K., Liu, X., Madhaiyan, M., Ji, L., Yang, L., Tang, C., Song, H., Kjelleberg, S., Cao, B. Influence of outer membrane c-type cytochromes on particle size and activity of extracellular nanoparticles produced by *Shewanella oneidensis*. *Biotechnol. Bioeng.*, 2013b;110(7):1831–1837.
110. Noah, N.F.M., Othman, N., and Jusoh, N. Highly selective transport of palladium from electroplating wastewater using emulsion liquid membrane process. *J. Taiwan Inst. Chem. Eng.*, 2016;64:134–141.
111. Okitsu, K., Iwasaki, K., Yobiko, Y., Bandow, H., Nishimura, R., Maeda, Y. Sonochemical degradation of azo dyes in aqueous solution: a new heterogeneous kinetics model taking into account the local concentration of OH radicals and azo dyes. *Ultrason. Sonochem.*, 2005;12:255–262.
112. Olthof, M., Eckenfelder, W.W. Coagulation of textile wastewater. *Text. Chem. Color.*, 1976;8:18–22.
113. Omajali, J.B., Gomez-Bolivar, J., Mikheenko, I.P., Sharma, S., Kayode, B., Al-Duri, B., Banerjee, D., Walker, M., Merroun, M.L., Lynne E. Macaskie, L.E. Novel catalytically active Pd/Ru bimetallic nanoparticles synthesized by *Bacillus benzeovorans*. *Sci Rep.*, 2019;9(1):4715.
114. Orozco, R.L., Redwood, M.D., Yong, P., Caldelari, I., Sargent, F., Macaskie, L.E. Towards an integrated system for bio-energy: Hydrogen production by *Escherichia coli* and use of palladium-coated waste cells for electricity generation in a fuel cell. *Biotechnol Lett.*, 2010;32(12):1837–1845.
115. Osawa, R.A., Carvalho, A.P., Monteiro, O.C., Oliveira, M.C., Florencio, M.H. Transformation products of citalopram: Identification, wastewater analysis and in silico toxicological assessment. *Chemosphere*, 2019;217:858–868.
116. Pandey, A., Shukla, P., Srivastava, P. Remediation of dyes in water using green synthesized nanoparticles (NPs). *IJPE*, 2020;6:68–84.
117. Pat-Espadas, A.M., Field, J.A., Otero-Gonzalez, L., Razo-Flores, E., Cervantes, F.J., Sierra-Alvarez, R. Recovery of palladium(II) by methanogenic granular sludge. *Chemosphere.*, 2016;144:745–753.
118. Pellerito, A., Ameen, S.M., Micali, M., Caruso, G. Antimicrobial substances for food packaging products: the current situation. *J. AOAC Int.*, 2018;101(4):942–947.
119. Previdello, B.A.F., Sibert, E., Maret, M., Soldo-Olivier, Y. Palladium electrodeposition onto Pt(100): Two-layer underpotential deposition. *Langmuir.*, 2017;33(9):2087–2095.
120. Qazi, F., Hussain, Z., Tahir, M.N. Advances in biogenic synthesis of palladium nanoparticles. *RSC Adv.*, 2016;6(65):60277–60286.
121. Quan, X., Sun, B., Xu, H. Anode decoration with biogenic Pd nanoparticles improved power generation in microbial fuel cells. *Electrochim Acta.*, 2015a;182:815–820.
122. Quan, X., Zhang, X., Xu, H. In-situ formation and immobilization of biogenic nanopalladium into anaerobic granular sludge enhances azo dyes degradation. *Water Res.*, 2015b;78:74–83.
123. Quan, X., Wang, X., Sun, Y., Li, W., Chen, L., Zhao, J. Degradation of diclofenac using palladized anaerobic granular sludge: Effects of electron donor, reaction medium and deactivation factors. *J. Hazard. Mater.*, 2019;365:155–163.
124. Quan, X., Wang, X., Zheng, Y., Li, W., Chen, L., Pei, Y. Effects of biogenic nanopalladium precipitation on the performance and microbial community structure of anaerobic granular sludge. *Sci Total Environ.*, 2020;705:135765.
125. Redwood, M.D., Deplanche, K., Baxter-Plant, V.S., Macaskie, L.E. Biomass-supported palladium catalysts on *Desulfovibrio desulfuricans* and *Rhodobacter sphaeroides*. *Biotechnol Bioeng.*, 2008;99(5):1045–1054.
126. Rezaei, S.S., Dehghanifard, E., Noorisepehr, M., Ghadirinejad, K., Kakavandi, B., Esfahani, A.R. Efficient clean-up of waters contaminated with diazinon pesticide using photo-decomposition of peroxymonosulfate by ZnO decorated on a magnetic core/shell structure. *J. Environ. Management.*, 2019;250:109472.
127. Rotaru, A.E., Jiang, W., Finster, K., Skrydstrup, T., Meyer, R.L. Nonenzymatic palladium recovery on microbial and synthetic surfaces. *Biotechnol Bioeng.*, 2012;109(8):1889–1897.
128. Safizadeh, F., Ghali, E., Houlachi, G. Electrocatalysis developments for hydrogen evolution reaction in alkaline solutions – A review. *Int. J. Hydrog. Energy.*, 2015;40(1):256–274.
129. Sahin, M., Gubbuk, I.H. Green synthesis of palladium nanoparticles and investigation of their catalytic activity for methylene blue, methyl orange and rhodamine B degradation by

- sodium borohydride. *React Kinetics Mech Catal.*, 2022;135:999–1010.
130. Sakimoto, K.K., Wong, A.B., Yang, P. Self-photosensitization of nonphotosynthetic bacteria for solar-to-chemical production. *Science.*, 2016;351(6268):74–77.
  131. Saldan, I., Semenyuk, Y., Marchuk, I., Reshetnyak, O. Chemical synthesis and application of palladium nanoparticles. *J. Mater. Sci.*, 2015;50(6):2337–2354.
  132. Saravanakumar, K., Mubarak Ali, D., Kathiresan, K., Thajuddin, N., Alharbi, N.S., Chen, J. Biogenic metallic nanoparticles as catalyst for bioelectricity production: A novel approach in microbial fuel cells. *Mater Sci Eng B.*, 2016;203:27–34.
  133. Sarmah, M., Neog, A.B., Boruah, P.K., Das, M.R., Bharali, P., Bora, U. Effect of substrates on catalytic activity of biogenic palladium nanoparticles in C–C cross-coupling reactions. *ACS Omega.*, 2019;4(2):3329–3340.
  134. Sathishkumar, M., Sneha, K., Kwak, I.S., Mao, J., Tripathy, S.J., Yun, Y.S. Phyto-crystallization of palladium through reduction process using *Cinnamom zeylanicum* bark extract. *J. Hazard. Mater.*, 2009;171(1):400–404.
  135. Sattayarat, V., Chanthad, C., Khemthong, P., Kuboon, S., Wanchaem, T., Phonyiem, M., Obata, M., Fujishige, M., Takeuchi, K., Wongwiriyan, W., Khanchaitit, P., Endo, M. Preparation and electrochemical performance of nitrogen-enriched activated carbon derived from silkworm pupae waste. *RSC Adv.*, 2019;9:9878–9886.
  136. Seh, Z.W., Kibsgaard, J., Dickens, C.F., Chorkendorff, I., Nørskov, J.K., Jaramillo, T.F. Combining theory and experiment in electrocatalysis: Insights into materials design. *Science.*, 2017;355(6321):eaad4998.
  137. Sen Gupta, P.S., Rana, M.K. Ivermectin, famotidine, and doxycycline: A suggested combinatorial therapeutic for the treatment of COVID-19. *ACS Pharm. Trans. Sci.*, 2020;3:1037-1038.
  138. Serpone, N., Terzian, R., Hidaka, H., Pelizzetti, E. Ultrasonic induced dehalogenation and oxidation of 2-, 3-, and 4-chlorophenol in air-equilibrated aqueous media. Similarities with irradiated semiconductor particulates. *J. Phys. Chem.*, 1994;98(10):2634–2640.
  139. Shafiee, S., Topal, E. When will fossil fuel reserves be diminished? *Energy Policy.*, 2009;37(1):181–189.
  140. Shaik, M.R., Ali, Z.J.Q., Khan, M., Kuniyil, M., Assal, M.E., Alkhatlan, H.Z., Al-Warthan, A., Siddiqui, M.R.H., Khan, M., Syed Farooq Adil, S.F. Green synthesis and characterization of palladium nanoparticles using *Origanum vulgare* L. extract and their catalytic activity. *Molecules (Basel, Switz)*. 2017;22(1):165.
  141. Sharmila, G., Farzana Fathima, M., Haries, S., Geetha, S., Manoj Kumar, N., Muthukumar, C. Green synthesis, characterization and antibacterial efficacy of palladium nanoparticles synthesized using *Filicium decipiens* leaf extract. *J. Mol. Struct.*, 2017;1138:35–40.
  142. Shi, L., Belchik, S.M., Plymale, A.E., Heald, S., Dohnalkova, A.C., Sybirna, K., Bottin, H., Squier, T.C., Zachara, J.M., Fredrickson, J.K. Purification and characterization of the [NiFe]-hydrogenase of *Shewanella oneidensis* MR-1. *Appl. Env. Microbiol.*, 2011;77(16):5584–5590.
  143. Shi, L., Richardson, D.J., Wang, Z., Kerisit, S.N., Rosso, K.M., Zachara, J.M., Fredrickson, J.K. The roles of outer membrane cytochromes of *Shewanella* and *Geobacter* in extracellular electron transfer. *Env Microbiol Rep.*, 2009;1(4):220–227.
  144. Siddiqi, K.S., Husen, A. Green synthesis, characterization and uses of palladium/platinum nanoparticles. *Nanoscale Res Lett.*, 2016;11(1):482.
  145. Siedlewicz, G., Białk-Bielinska, A., Borecka, M., Winogradow, A., Stepnowski, P., Pazdro, K. Presence, concentrations and risk assessment of selected antibiotic residues in sediments and near-bottom waters collected from the Polish Coastal Zone in the Southern Baltic Sea—Summary of 3 years of studies. *Mar. Pollut. Bull.*, 2018;129:787–801.
  146. Silva, L., Moreira, C., Curzio, B., da Fonseca, F. Micropollutant removal from water by membrane and advanced oxidation processes—A review. *J. Water Resour. Prot.*, 2017;9:411–431.
  147. Singh, A., Gautam, P.K., Verma, A., Singh, V., Shivapriya, P.M., Shivalkar, S., Sahoo, A.K., Samanta, S.K. Green synthesis of metallic nanoparticles as effective alternatives to treat antibiotics resistant bacterial infections: A review. *Biotechnol Rep (Amst)*, 2020;25:e00427.
  148. Sivamaruthi, B.S., Ramkumar, V.S., Archunan, G., Chaiyasut, C., Suganthy, N. Biogenic synthesis of silver palladium bimetallic nanoparticles from fruit extract of *Terminalia chebula* – In vitro evaluation of anticancer and antimicrobial activity. *J. Drug Delivery Sci. Technol.*, 2019;51:139–151.
  149. Stackelberg, P.E., Gibs, J., Furlong, E.T., Meyer, M.T., Zaugg, S.D., Lippincott, R.L. Efficiency of conventional drinking-water-treatment processes in removal of pharmaceuticals and other organic compounds. *Sci. Total Environ.*, 2007;377:255–272.
  150. Statgraphics Centurion XV, software, StatPoint Inc, Statgraphics Centurion XV, Herndon, VA, USA, 2005.
  151. Suja, E., Nancharaiya, Y.V., Venugopalan, V.P. Biogenic nanopalladium production by self-immobilized granular biomass: application for contaminant remediation. *Water Res.*, 2014;65:395–401.
  152. Świątkowski, A. Industrial carbon adsorbents. In: Dąbrowski A, editor. *Studies in surface science and catalysis*. Lublin, Poland: Elsevier; 1999;120:69–94.
  153. Tahernia, M., Mohammadifar, M., Feng, S., Choi, S., editors. Biogenic palladium nanoparticles for improving bioelectricity generation in microbial fuel cells. 2020 IEEE 33rd International Conference on Micro Electro Mechanical Systems (MEMS); Jan. 2020:18–22.
  154. Tamma, P.D., Avdic, E., Li, D.X., Dzintars, K., Cosgrove, S.E. Association of adverse events with antibiotic use in hospitalized patients. *JAMA Intern. Med.*, 2017;177:1308–1315.
  155. Tan, L., Li, L.Y., Ashbolt, N., Wang, X.L., Cui, Y.X., Zhu, X., Xu, Y., Yang, Y., Mao, D.Q., Luo, Y. Arctic antibiotic resistance gene contamination, a result of anthropogenic activities and natural origin. *Sci. Total Environ.*, 2018;621:1176–1184.
  156. Thapa, B.S., Kim, T., Pandit, S., Song, Y.E., Afsharian, Y.P., Rahimnejad, M., Kim, J.R., Oh, S.-E. Overview of electroactive microorganisms and electron transfer mechanisms in microbial electrochemistry. *Bioresour Technol.*, 2022;347:126579.
  157. The American Society of Health-System Pharmacists. Ofloxacin. Archived from the original on 28 December 2016. Retrieved 8 December 2016.
  158. Tong, C., Zhuo, X., Guo Y. Occurrence and risk assessment of four typical fluoroquinolone antibiotics in raw and treated sewage and in receiving waters in Hangzhou, China. *J. Agric. Food Chem.*, 2011;59(13):7303–7309.
  159. Tong, S., Pan, J., Lu, S., Tang, J. Patient compliance with antimicrobial drugs: a Chinese survey. *Am. J. Infect. Control.*, 2018;46:E25–E29.
  160. Tuo, Y., Liu, G., Dong, B., Yu, H., Zhou, J., Wang, J., Jin, R. Microbial synthesis of bimetallic PdPt nanoparticles for catalytic reduction of 4-nitrophenol. *Env. Sci. Pollut. Res. Int.*, 2017;24(6):5249–5258.
  161. Vallee, B.L., Ulmer, D.D. Biochemical effects of mercury, cadmium, and lead. *Annu. Rev. Biochem.*, 1972;41(10):91–128.

162. Van Nevel, S., Hennebel, T., Verschuere, S., De Corte, S., Boon, N., Verstraete, W. Palladium nanoparticles produced by fermentatively grown bacteria as catalyst for diatrizoate removal with biogenic hydrogen. *Communications in Agricultural and Applied Biological Sciences*, 2011;76(1):185-188.
163. Venkateswaran, K.; Moser, D. P.; Dollhopf, M. E.; Lies, D. P.; Saffarini, D. A.; MacGregor, B. J.; Ringelberg, D. B.; White, D. C.; Nishijima, M.; Sano, H.; Burghardt, J.; Stackebrandt, E.; Neelson, K. H. (1999). Polyphasic taxonomy of the genus *Shewanella* and description of *Shewanella oneidensis* sp. nov. *International Journal of Systematic Bacteriology*, 1999;49(2): 705–724.
164. Verlicchi, P., Galletti, A., Masotti, L. Management of hospital wastewaters: the case of the effluent of a large hospital situated in a small town. *Water Sci. Technol.*, 2010;61(10):2507–2519.
165. Vijayaraghavan, K., Ashokkumar, T. Plant-mediated biosynthesis of metallic nanoparticles: A review of literature, factors affecting synthesis, characterization techniques and applications. *J. Environ. Chem. Eng.*, 2017;5(5):4866–4883.
166. Villegas-Guzman, P., Silva-Agredo, J., Florez, O., Giraldo-Aguirre, A.L., Pulgarin, C., Torres-Palma, R.A. Selecting the best AOP for isoxazolyl penicillins degradation as a function of water characteristics: effects of pH, chemical nature of additives and pollutant concentration. *J. Environ. Manage.*, 2017;190:72–79.
167. Wang, W., Zhang, B., He, Z. Bioelectrochemical deposition of palladium nanoparticles as catalysts by *Shewanella oneidensis* MR-1 towards enhanced hydrogen production in microbial electrolysis cells. *Electrochim Acta.*, 2019;318:794–800.
168. Wang, P.T., Song, Y.H., Fan, H.C., Yu, L. Bioreduction of azo dyes was enhanced by in-situ biogenic palladium nanoparticles. *Bioresour. Technol.*, 2018;266:176-180.
169. Wang, J., Hao, J., Liu, D., Qin, S., Chen, C., Yang, C., Liu, Y., Yang, T., Fan, Y., Chen, Y., Lei, W. Flower stamen-like porous boron carbon nitride nanoscrolls for water cleaning. *Nanoscale.*, 2017a;9:9787-9791.
170. Wang, X., Wang, A., Lu, M., Ma, J. Synthesis of magnetically recoverable Fe<sup>0</sup>/graphene-TiO<sub>2</sub> nanowires composite for both reduction and photocatalytic oxidation of metronidazole. *Chem. Eng. J.*, 2017b;337:372–384.
171. Wang, W., Zhu, Q., Dai, Q., Wang, X. Fe doped CeO<sub>2</sub> nanosheets for catalytic oxidation of 1,2-dichloroethane: Effect of preparation method. *Chem. Eng. J.*, 2017c;307:1037-1046.
172. Watanabe, K. Recent developments in microbial fuel cell technologies for sustainable bioenergy. *J. Biosci. Bioeng.*, 2008;106(6):528–536.
173. Wei, Z., Liu, J., Shanguan, W. A review on photocatalysis in antibiotic wastewater: Pollutant degradation and hydrogen production. *Chinese J. Catal.*, 2020;41(10):1440-1450.
174. Wiatrowski, H.A., Ward, P.M., Barkay, T. Novel reduction of mercury (II) by mercury-sensitive dissimilatory metal reducing bacteria. *Environmental Science and Technology*, 2006;40(21):6690–6696.
175. Wu, G., Li, N., Mao, Y., Zhou, G., Gao, H. Endogenous generation of hydrogen sulfide and its regulation in *Shewanella oneidensis*. *Front Microbiol.*, 2015;6(374):374.
176. Wu, R., Tian, X., Xiao, Y., Ulstrup, J., Mølager Christensen, H.E., Zhao, F., Zhang, J. Selective electrocatalysis of biofuel molecular oxidation using palladium nanoparticles generated on *Shewanella oneidensis* MR-1. *J. Mater. Chem. A.*, 2018;6(23):10655–10662.
177. Wu, X., Zhao, F., Rahunen, N., Varcoe, J.R., Avignone-Rossa, C., Thumser, A.E., Slade, R.C.T. A Role for microbial palladium nanoparticles in extracellular electron transfer. *Angew. Chem. Int. Ed.*, 2011;50(2):427–430.
178. Xiao, Y., Chang, H., Jia, A., Hu, J. Trace analysis of quinolone and fluoroquinolone antibiotics from wastewaters by liquid chromatography–electrospray tandem mass spectrometry. *J. Chromatogr. A.*, 2008;1214(1):100-108.
179. Xiong, L., Zhang, X., Huang, Y.-X., Liu, W.-J., Chen, Y.-L., Yu, S.-S., Hu, X., Cheng, L., Liu, D.-F., Yu, H.-Q. Biogenic synthesis of Pd-based nanoparticles with enhanced catalytic activity. *ACS Appl Nano Mater.* 2018;1(4):1467–1475.
180. Xu, H., Shang, H., Wang, C., Du, Y. Recent progress of ultrathin 2D Pd-based nanomaterials for fuel cell electrocatalysis. *Small.*, 2021;17(5):2005092.
181. Xu, H., Tan, L., Cui, H., Xu, M., Xiao, Y., Wu, H., Dong, H., Liu, X., Qiu, G., Xie, J. Characterization of Pd(II) biosorption in aqueous solution by *Shewanella oneidensis* MR-1. *J. Mol. Liq.*, 2018;255:333–340.
182. Xu, C., Nasrollahzadeh, M., Selva, M., Issaabadi, Z., Luque, R. Waste-to-wealth: biowaste valorization into valuable bio(nano)materials. *Chem. Soc. Rev.*, 2019;48:4791–4822.
183. Yagub, M.T., Sen, T.K., Afroze, S., Ang, H.M. Dye and its removal from aqueous solution by adsorption: a review. *Adv. Colloid Interface Sci.*, 2014;209:172-184.
184. Yang, Z.-N., Hou, Y.-N., Zhang, B., Cheng, H.-Y., Yong, Y.-C., Liu, W.-Z., Han, J.-L., Liu, S.-J., Wang, A.-J. Insights into palladium nanoparticles produced by *Shewanella oneidensis* MR-1: Roles of NADH dehydrogenases and hydrogenases. *Env. Res.*, 2020;191:110196.
185. Yang, L., Zhu, Y.-J., He, G., Li, H., Tao, J.-C. multifunctional photocatalytic filter paper based on ultralong nanowires of the calcium-alendronate complex for high-performance water purification. *ACS Appl. Mater. Interfaces.*, 2022;14:9464-9479.
186. Yang, X., Chen, Z., Zhao, W., Liu, C., Qian, X., Zhang, M., Wei, G., Khan, E., Hau Ng, Y., Sik Ok, Y. Recent advances in photodegradation of antibiotic residues in water. *Chem. Eng. J.*, 2021;405:126806.
187. Yin, J., Gao, H. Stress responses of *Shewanella*. *Int. J. Microbiology.*, 2011;2011:863623.
188. Yong, P., Rowson, N.A., Farr, J.P., Harris, I.R., Macaskie, L.E. Bioreduction and biocrystallization of palladium by *Desulfovibrio desulfuricans* NCIMB 8307. *Biotechnol. Bioeng.*, 2002;80(4):369–379.
189. Yuan, H., He, Z. Platinum group metal-free catalysts for hydrogen evolution reaction in microbial electrolysis cells. *Chem. Rec.*, 2017;17(7):641–652.
190. Zaher, U., Bouvier, J., Steyer, J.P., Vanrolleghem, P. Titrimetric monitoring of anaerobic digestion: VFA, alkalinities and more. *Proceedings of 10th IWA World Congress on Anaerobic Digestion (AD10)*; 2004;1.
191. Zar, J.H. *Biostatistical analysis*, Prentice-Hall, Englewood Cliffs, 1984.
192. Zhang, C., Li, Y., Shuai, D., Shen, Y., Xiong, W., Wang, L. Graphitic carbon nitride (g-C<sub>3</sub>N<sub>4</sub>)-based photocatalysts for water disinfection and microbial control: A review. *Chemosphere*, 2019;214:462-479.
193. Zhang, L.-H., He, Y.-W., Chen, M., Gao, M., Qiu, T.-L., Wang, X.-M. Pollution characteristics of antibiotic resistant bacteria from atmospheric environment of animal feeding operations. *Huan. Jing. Ke. Xue.*, 2016;37:4531-4537.
194. Zheng, Z., Cao, H., Meng, J., Xiao, Y., Ulstrup, J., Zhang, J., Zhao, F., Engelbrekt, C., Xiao, X. Synthesis and structure of a two-dimensional palladium oxide network on reduced graphene oxide. *Nano Lett.*, 2022;22(12):4854–4860.
195. Zhong, Y., Han, L., Yin, X., Li, H., Fang, D., et al. (2018). Three dimensional functionalized carbon/tin(IV) sulfide biofoam for photocatalytic purification of chromium(VI)-containing wastewater. *ACS Sustain. Chem. Eng.*, 6:10660-10667.

196. Zhou, W.P., Lewera, A., Larsen, R., Masel, R.I., Bagus, P.S., et al. (2006). Size effects in electronic and catalytic properties of

unsupported palladium nanoparticles in electrooxidation of formic acid. *J. Phys. Chem. B.*, 110(27):13393–13398.



This work is licensed under Creative Commons Attribution 4.0 License

To Submit Your Article Click Here:

[Submit Manuscript](#)

DOI: [10.31579/2690-4861/300](https://doi.org/10.31579/2690-4861/300)

**Ready to submit your research? Choose Auctores and benefit from:**

- fast, convenient online submission
- rigorous peer review by experienced research in your field
- rapid publication on acceptance
- authors retain copyrights
- unique DOI for all articles
- immediate, unrestricted online access

At Auctores, research is always in progress.

Learn more <https://auctoresonline.org/journals/international-journal-of-clinical-case-reports-and-reviews->